



University of
Stavanger

Faculty of Science and Technology

MASTER'S THESIS

Study program/ Specialization: Offshore technology / Marine and Subsea Technology	Spring semester, 2014 Open access
Writer: Kjetil Lund Fossli (Writer's signature)
Faculty supervisor: Professor Arnfinn Nergaard	
Thesis title: A study of fracture mechanisms when exposed to hydrostatic loads	
Key words: Fracture mechanics, Bridgman, Pinch-off effect, Effective tension theory.	Pages: Stavanger, Date/year

Preface:

This thesis is written as a final closure for my master degree program in Offshore Technology, Subsea Technology at the University of Stavanger. Thesis was conducted from January to June 2014.

Thesis main topic is the Bridgman experiment, a special experiment with an unexpected result.

For me as a student, there has been many new challenges during the work on this thesis. As there is no exact solution to the problem, I had to read and listen to the opinions and references with more criticism than normal. This made the thesis more interesting. I enjoyed the meeting with people, listening and discussing the possible solutions, asking questions and explain the observations during this spring semester.

I would like to thank my supervisor Arnfinn Nergaard for his help and good support, for using his papers for reference. I would also like to mention other people helping. Samdar Kakay (UiS) for help during tension experiments, Ingunn Cecilie Oddsen (UiS) for help with microscope. Bernt Aadnøy (UiS) for his explanation and shearing of papers. Hirpa Gelgele Lemu (UiS) for his time and explanations and Anne Serine Ognedal (NTNU) for emails and discussion. Also Kenneth Alasdair Macdonald (Statoil) and all the other people I met or emailed where I got explanations and ideas.

Kjetil Lund Fossli

Summary:

Bridgman experiment is an experiment that was conducted by Bridgman in 1912. This simple experiment consists of a rod going all the way through a pressure vessel. When pressurizing the vessel, the rod is loaded on the curved surface and when pressure get high enough, the rod fractures.

There are still disagreement on the reason for fracture. Two explanations tend to stand against each other. One side explaining the fracture with use of the effective tension theory and the other side with use of Von Mises criterion and Poisson ratio. With examples from calculation of buoyancy, the two sides are explained and understood. Both sides with experiments differentiating them and their arguments. Then the theory on effective tension is elaborated by super positioning and explained.

During the thesis, experiments were conducted. Bridgman experiment, bending experiment and tension experiment. All rods were cut down in size and photographed in SEM (Scanning Electron Microscope) to have a closer look at the fracture surfaces. It was shown that the fracture surface from Bridgman experiment is a fracture surface of tension. Results were discussed with several experts and feedback from both sides were discussed. Further investigations in three different softwares, AutoCAD Inventor, OpenFOAM and Ansys. Neither of the softwares show axial tension in the rods during pressure loading. Experts on the softwares were contacted and defended their software.

Table of contents

	Page
Preface	2
Summary	3
List of tables, figures and pictures:	
Figures.....	6
Tables.....	6
Pictures.....	7
Nomenclature and abbreviations	8
Chapter 1. Introduction	9
1.1 Outline of the thesis.....	10
1.2 Objectives.....	11
Chapter 2. Two schools	12
2.1 School I: Compression.....	12
2.2 School II: Tension.....	14
Chapter 3. Analogy to understanding bouyancy	17
3.1 School I: Piston method.....	17
3.2 School II: Volumetric method.....	18
3.3 Experiments supporting different understandings of bouyancy..	18
3.3.1 Favoring piston method of calculating bouyancy.....	18
3.3.2 Favoring volumetric method of calculating bouyancy.....	20
Chapter 4. Body forces under hydrostatic load	23
4.1 Axial forces.....	23
4.1.1 Solid submerged body.....	23
4.1.2 Pipes.....	24
4.2 Effective stresses.....	25
4.3 Tresca, Von Mises and Poisson.....	27
4.4.1 Tresca criterion.....	27
4.4.2 Von Mises criterion.....	28
4.4.3 Poisson ratio.....	30
Chapter 5. Fracture mechanics of plastic materials	31
5.1 Fracture mechanics.....	31

	Page
Chapter 6. Looking at fracture surfaces from Bridgman experiment.....	34
6.1 Bridgman’s observations and fracture model alternatives.....	34
6.1.1 Bridgman’s observations.....	34
6.1.2 Fracture model alternatives.....	35
6.2 Introduction.....	36
6.3 Materials.....	36
6.4 Bridgman experiment.....	37
6.4.1 Bridgman experiment results.....	39
6.4.2 Bridgman experiment SEM results.....	42
6.5 Bending experiment.....	42
6.5.1 Bending experiment results.....	43
6.5.2 Bending experiment SEM results.....	43
6.6 Tension loading experiment.....	44
6.6.1 Tension loading experiment results.....	45
6.6.2 Tension loading experiment SEM results.....	46
6.7 Discussion.....	46
6.7.1 Bridgman experiment discussion.....	46
6.7.2 Moment experiment discussion.....	48
6.7.3 Tension loading experiment discussion.....	49
6.8 Experiment summation.....	50
6.9 Comments to experiments.....	51
Chapter 7. The software paradox.....	54
7.1 Ansys.....	54
7.2 Autodesk Inventor.....	54
7.3 Openfoam.....	55
Chapter 8. Results summarized.....	57
Chapter 9. Summation and conclusion.....	58
References.....	60
Appendix:	
Appendix A.....	63
Appendix B.....	69
Appendix C.....	71
Appendix D.....	77
Appendix E.....	79
Appendix F.....	81

Figures

	Page
Fig 2-1: Pressure on curved surface.....	12
Fig 2-2: Nergaard, A. Bridgman paradox.....	14
Fig 2-3: Nergaard, A. Tri step paradox.....	15
Fig 2-4: Nergaard, A. Tri step paradox.....	16
Fig 2-5: Nergaard, A. Tri step paradox.....	16
Fig 3-1: Goins experiment.....	19
Fig 3-2: Cylinder on seafloor.....	20
Fig 3-3: Cylinder on seafloor, piston method.....	21
Fig 3-4: Cylinder on seafloor, volumetric method.....	21
Fig 4-1: Effective stress in submerged body.....	23
Fig 4-2: Effective stress in submerged pipe.....	25
Fig 4-3: Stress cube.....	26
Fig 4-4: Stress and shear cube.....	26
Fig 4-5: Tresca curve.....	27
Fig 4-6: Tresca and Von Mises 3D curves.....	28
Fig 5-1: Tension failure types.....	32
Fig 5-2: Void types.....	32

Tables

	Page
Tab 6-1: Bridgman experiment, pressure and material strengths.....	39
Tab 6-2: Bridgman experiment, diameter and lengths.....	39
Tab 6-3: Bridgman experiment, strain.....	40
Tab 6-4: Tension experiment, load and material strengths.....	45
Tab 6-5: Tension experiment, strain.....	45
Tab 6-6: Bridgman tension material strength, volumetric.....	47
Tab 6-7: Bridgman tension material strength, piston.....	47
Tab 6-8: Bridgman vs. Tension material strength, volumetric.....	51
Tab 6-9: Bridgman vs. Tension material strength, piston.....	51

Pictures

	<i>Page</i>
<i>Pic 5-1: Crazing.....</i>	<i>33</i>
<i>Pic 6-1: Bridgman`s picture.....</i>	<i>34</i>
<i>Pic 6-2: PMMA.....</i>	<i>36</i>
<i>Pic 6-3: POM-C.....</i>	<i>36</i>
<i>Pic 6-4: POM-C.....</i>	<i>37</i>
<i>Pic 6-5: PA-6.....</i>	<i>37</i>
<i>Pic 6-6: Bridgman pressure vessel.....</i>	<i>38</i>
<i>Pic 6-7: High pressure unit.....</i>	<i>39</i>
<i>Pic 6-8: PA-6 rod fail.....</i>	<i>40</i>
<i>Pic 6-9: PMMA rod crazing.....</i>	<i>40</i>
<i>Pic 6-10: PMMA fracture surface.....</i>	<i>41</i>
<i>Pic 6-11: POM-C fracture surface.....</i>	<i>41</i>
<i>Pic 6-12: Random fracture location.....</i>	<i>42</i>
<i>Pic 6-13: PMMA moment fracture.....</i>	<i>43</i>
<i>Pic 6-14: POM-C moment fracture.....</i>	<i>43</i>
<i>Pic 6-15: Tension machine.....</i>	<i>44</i>
<i>Pic 6-16: PMMA tension fracture.....</i>	<i>45</i>
<i>Pic 6-17: Voids.....</i>	<i>48</i>
<i>Pic 6-18: POM-C fracture surfaces. Sanded(l) and turned(r).....</i>	<i>49</i>
<i>Pic 6-19: PMMA fracture propagation.....</i>	<i>50</i>

Nomenclature and abbreviations:

Nomenclature :

σ – Stress tensor
 $\sigma_1, \sigma_2, \sigma_3$ – principal stresses
 σ_d – Deviatoric stress
 σ_e – Effective stress
 σ_h – Hydrostatic stress
 σ_p – Principal stress
 σ_{VM} – Von Mises stress
 $\epsilon_{xx}, \epsilon_{yy}, \epsilon_{zz}$ – strain
 ν – Poisson ratio
 ϕ – Angle
 ρ – Density
 τ – Shear stress
 A, A_e – Outer area
 a, a_i – Inner area
 E – Modulus of elasticity
 F_B – Bouyancy force
 g – gravitational acceleration
 G – Shear modulus
 I – Stress invariants
 J – Deviatoric stress invariants
 K – Bulk modulus
 P – Pressure
 R, R_e – Outer radius
 r, r_i – inner radius
 T – Tension
 T_e – Effective tension
 T_{TW} – True wall tension
 U_0 – Total strain energy density
 U_D – Change due to disortion
 U_v – Volumetric change
 V – Volume
 W – Weight
 W_a – Apparent weight
 W_f – Fluid weight
 W_t – True weight
 Y – Yield limit

Abbreviations :

PA-6 – Polycaprolactam (Nylon-6)
PMMA – Poly Methyl Metachrylate
POM – Polyacetal (Acetal Copolymer)
SEM – Scanning Electron Microscope

1. Introduction

Percy Williams Bridgman is a man who lived in America at the start of 20th century, known for his work with high pressure. Around 1912, he conducted experiments on "Breaking tests under Hydrostatic Pressure and Conditions of Rupture" [12]. Several of his experiments appeared to be of types not observed before. Still, Bridgman was not attempting to develop new theory, just describing and discussing the experiments themselves.

One of his experiments, an experiment on the pinch-off effect, consist of a rod that passes completely through a pressure vessel. The vessel is sealed at both ends with sealing rings and connected to a pressure pump. Pressure is applied to the fluid in the annular space between the rod and the inner wall of the vessel so that the rod is loaded on the curved surface only. The result of the experiment is that the rod fractures. The pieces are expelled through the sealing rings.

Bridgman was referring to this result as pinching-off effect. Further he assumed no stress in the longitudinal axis of the rod, neglecting the friction from the sealing rings. Experiments with different materials revealed different types of fracture. Fracture mechanism were not explained. The Bridgman experiment became a Bridgman paradox.

In 2013, Morten Reve wrote his masters thesis "Understanding of buoyancy in drill pipe and risers" [13.]. He wrote about how axial forces are calculated in risers exposed to hydrostatic radial pressure on the surface. As part of this, he studied the effective tension theory outlined by Charles P. Sparks who is the author of "Fundamentals of marine riser mechanics" [5.]. Sparks is often referred to when it comes to effective tension theory, including the offshore standards [25.]. With the use of his theory, Sparks states that "a suspended riser will see a buoyancy force equal to the weight of the fluid displaced, which for a vertical riser of uniform cross section is equal to the pressure x area ($P_e A_e$) acting at the riser lower end. Note, however, that the buoyancy force acts at the centroid of the submerged volume, at the mid height of the submerged length, not at the riser lower end."

With the idea that the effective tension concept still works for horizontal pipes, the Bridgman

experiment was conducted. The experiments resulted in the pinch-off effect, just as expected. The rods were expelled out of the pressure vessel, a fracture occurred at pressures around the tensile strength of the material. A discussion developed, emails were sent around trying to explain what was happening. At a stage, there was even suggested that Newtons laws did not apply. One year later there are still disagreement among experts on the fracture mechanism on the Bridgman experiment. Explanations on the fracture can be split into two sides, two schools with different opinions and logics to explain the Bridgman experiment and how the fracture develops [2.].

During the past 100 years that have passed since Bridgman put up his experiment there has been a rapid development of knowledge, techniques, equipment and technology. This technology can be used to support calculations and experiments that can shed light on new discoveries or modify the old ones. Some of the strongest and most used tool we have are the softwares that can model and simulate experiments virtually. The Bridgman experiment was modeled in OpenFOAM Ansys and Autodesk Inventor to find more answers and maybe a reason. Non of the softwares could clearly identify a reason for the fracture. Could it be, that after 100 years, we still have a paradox?

1.1 Outline of the thesis

2. Two schools. This chapter will show the reader there are two sides of understanding Bridgman experiment and how the pinch-off is explained.
3. Analogy to understanding of buoyancy. Reader will be introduced to how the internal forces created by buoyancy is calculated. For better understanding the differences in the way of thinking between the two schools.
4. Body forces under hydrostatic load. This is a chapter about how forces from hydrostatic pressure is acting on submerged bodies and how this will affect the dimensioning stresses.
5. Mechanics of plastic materials. Fracture mechanics in plastic rods as used in the Bridgman experiment.
6. Looking at fracture surfaces from Bridgman experiment. Three different experiments are conducted for a closer look at the fracture surface through SEM (Scanning Electron Microscope).

7. The software paradox. Contains results from modeling Bridgman experiment in three different and well known softwares to explain the internal forces in the rods.

1.2 Objectives

This thesis is written to study and analyze the pinch-off effect in the Bridgman experiment. By studying the fracture mechanics with modern knowledge and technique, the aim is to find evidence for a solution that converges the different views.

- Use the new criteria on the classic mechanics developed the past century.
- Introduce the theory on effective stress related to hydrostatics.
- Study the fracture in Bridgman experiment with electron microscope.
- Collect opinions by talking to experts and listen to their experience, opinions and statements.
- Model and simulate Bridgman experiment in software analysis tools for mechanical behavior.

2. Two schools

There are two different main opinions on how the rod fails in the Bridgman experiment [2]. One is more widely supported than the other. School I is into compression and how the pressurized rod will fracture due to big variation in stress. School II is explaining the fracture with support from the effective tension theory. The tension effect is also demonstrated through a three step symmetry explanation.

2.1 School I: Compression

When the rod is loaded on curved surface, the rod will shrink in diameter and expand in length. This will create a fictitious tension force in the axial direction. When the strain and stress differences grow too big, the rod ruptures at Von Mises stress.

Material will tend to squeeze like glue out of a tube. Von Mises criterion will apply.

In the Bridgman experiment we have this model of the situation [Fig 3.1].

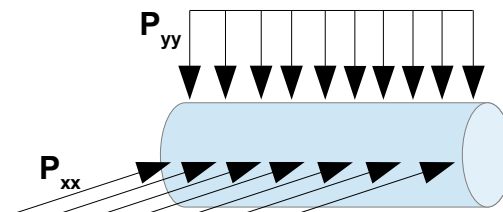


Fig 2-1: Pressure on curved surface

Finding the principal stresses:

$$\sigma_{xx} = -P$$

$$\sigma_{yy} = -P$$

$$\sigma_{1,2} = \frac{\sigma_{xx} + \sigma_{yy}}{2} \pm \sqrt{\left(\frac{\sigma_{xx} - \sigma_{yy}}{2}\right)^2 + \tau_{xy}^2} \quad \text{Equation 3.1}$$

$$\sigma_{1,2} = \frac{-P - P}{2} \pm \sqrt{\left(\frac{-P + P}{2}\right)^2 + 0^2} = \frac{-P - P}{2} \pm 0 = -P$$

$$\sigma_{1,2} = -P$$

sqrt yield criterion:

$$\sigma_{VM} = \sqrt{\frac{1}{2} [(\sigma_1 - \sigma_2)^2 + (\sigma_2 - \sigma_3)^2 + (\sigma_3 - \sigma_1)^2]} \quad \text{Equation 3.2}$$

$$\sigma_{VM} = \sqrt{\frac{1}{2} [(-P + P)^2 + (-P - 0)^2 + (0 + P)^2]} = \sqrt{\frac{1}{2} (P^2 + P^2)} = P$$

$$\underline{\sigma_{VM} = P}$$

Meaning the rod will fracture at a stress equal to the pressure in the vessel.

Equivalent tension in the rod can also be found [31.]:

For bridgman experiment , rod under load :

$$\epsilon_{zz} E = \sigma_{zz} - \nu (\sigma_{xx} + \sigma_{yy}) \quad \text{Equation 3.3}$$

$$\sigma_{zz} = 0$$

$$-P = \sigma_{xx} = \sigma_{yy}$$

$$\epsilon_{zz} = -2\nu \frac{-P}{E}$$

$$\epsilon_{zz} = \frac{2\nu P}{E}$$

Now turn this example around. Finding the equivalent stress if we have strain :

$$\sigma_{zz} = \epsilon_{zz} E \quad \text{Equation 3.4}$$

$$\sigma_{zz} = 2\nu P$$

This is the most popular explanation. It does not contradict the observations. It could be said that there should be a less abrupt fracture than what the picture from Bridgman's experiment is showing. The PA-6 rod show indications on a more expected cross sectional decrease like a parabola over the total inner length of the pressure vessel.

2.2 School II: Tension

Example 1: Hydrostatic pressure loading, the three step solution.

Professor Arnfinn Nergaard put up this as an understanding of the problem:

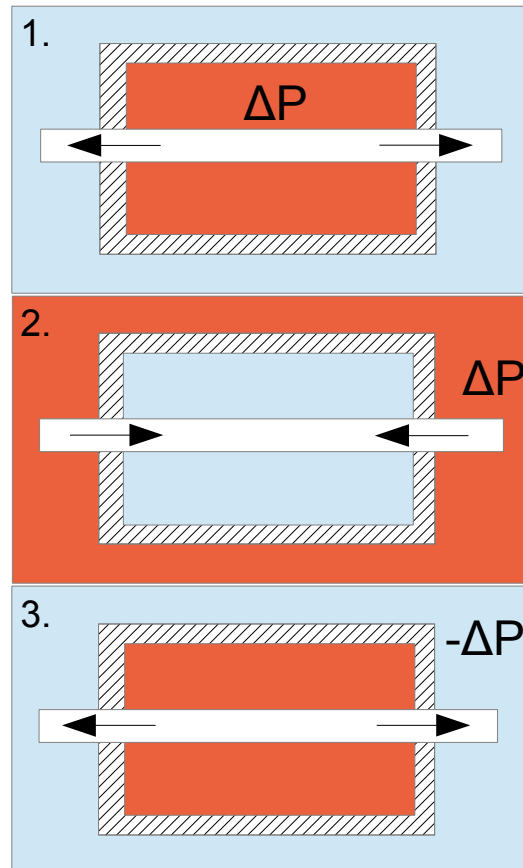


Fig 2-2: Nergaard, A. Bridgman paradox

Step 1: Faced with the seemingly trivial physical problem with a pressurized vessel with a bar protruding the vessel walls through sealing glands, most people opt for solution 1; no resulting axial force; $T = 0$.

Step 2: By reversing the pressure, there is 100% agreement that solution 2 gives the right answer. A compression force corresponding to the overall piston effect.

Step 3: Most people agree that lowering external pressure to negative gives a suction force and corresponding tension in the piston of $T = \Delta pA$.

Then, the question is: Is not step 3 identical to step 1?

A lot of people do not agree that step 1 equals step 3. They say the big and important difference is that the load is applied in radial direction in step 1 and at the ends in step 3.

Example 2: Pipe through a pressure vessel, another three step solution

Another example from Professor Arnfinn Nergaard is this pipe through a pressure vessel.

Step 1.

A tube is subjected to an external pressure [Fig 3-3]. To calculate the axial force in the pipe, most people will come with the solution:

a)

$$T = \Delta P (A - a) \tag{Equation 3.5}$$

Others may find this as a solution:

b) $T = \Delta P A$

$$\tag{Equation 3.6}$$

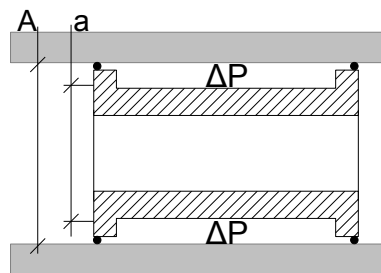


Fig 2-3: Nergaard, A. Tri step paradox.

$$T = \Delta P (A - a) + \Delta P_e \cdot A_e \tag{Equation 3.7}$$

Where:

$$A_e = a$$

$$P_e = \Delta P$$

$$T = \Delta P (A - a) + \Delta P a = \Delta P A - \Delta P a + \Delta P a$$

$$T = \Delta P A$$

Step 2.

Most people will agree that the solution is the same if we have a solid piston.

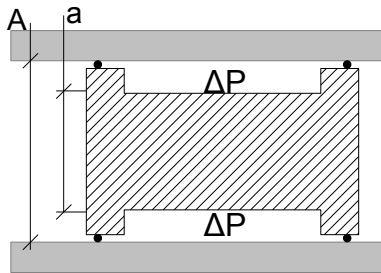


Fig 2-4: Nergaard, A. Tri step paradox.

$$T = \Delta P(A - a) + \Delta P_e \cdot A_e$$

Equation 3.8

Where:

$$A_e = a$$

$$P_e = \Delta P$$

$$T = \Delta P(A - a) + \Delta P a = \Delta P A - \Delta P a + \Delta P a$$

$$T = \Delta P A$$

Step 3.

ΔP is nothing but a difference in the pressure. By selecting an opposite pressure on the outside of the piston, the problem is equal to the above, but more people agree that the tension in the piston is calculated as 1.b) :

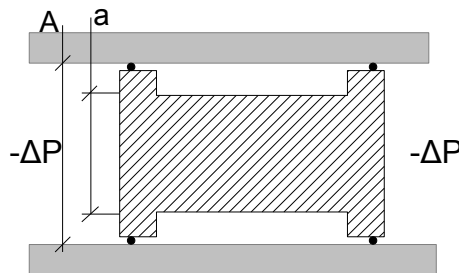


Fig 2-5: Nergaard, A. Tri step paradox.

$$T = \Delta P A$$

Same result as 1. and 2.

The opposite but same problem as 2.

Again, many people do not agree that step 1 equals step 3. Reason is the same. The load is applied in radial direction in step 1 and at the ends in step 3.

3. Analogy to the understandings of buoyancy

In Bridgman experiment, the rod is only subjected to hydrostatic forces on the curved surface. In School I, this does mean that there can act axial forces in the rod. School II thinks different, there can not occur axial forces. This chapter will look into the arguments and mathematics that are used to argue why and why not there are axial forces in bodies loaded orthogonally to the axial direction by using the calculation of buoyancy as example.

3.1 School I: Piston method

Buoyancy is calculated as the difference of pressure over the body. The pressure on a body method is easy to understand, we can see where the forces are and where the direction of floating is coming from. Its a simple calculation for simple surfaces, but will easily get complicated as the surface get curved.

$$F_B = \iint_S p \hat{n} dS \quad \text{Equation 4.1}$$

Where:

F_B – Bouyancy force

dS – Area subjeced to pressure

p – Pressure

\hat{n} – Normal vector on area

This can also be written as an integral of volume by using the Gauss divergence theorem.[20]

$$F_B = \iint_S p \hat{n} dS$$

$$p(z) = -\rho g z$$

$$F_B = \iint_S p \hat{n} dS = -\rho g \iint_S z \hat{n} dS$$

By using Gauss theorem, we have:

$$\iint_S G \hat{n} dS = \iiint_V \Delta G dV = \rho g \iiint_V dV$$

Which is:

$$F_B = \rho g V$$

This conversion by Gauss divergence theorem is only legal when there is an area around the body which is of the fluid. So if the body is connected to any surface on any side that differentiates in pressure over the body, the body is not subjected to true buoyancy. It will not float to surface. Even the thinnest surface is enough, so everything placed on a wet floor is subjected to buoyancy.

3.2 School II: Volumetric method

The volumetric method of calculating buoyancy is often less complicated as you only need to calculate the volume. This is more like how Archimedes said it and probably also how he experienced it. Archimedes said: "A body immersed in a fluid experiences a vertical buoyant force equal to the weight of the fluid that it displaces" [1].

Buoyancy is calculated as:

$$F_B = \rho g V \qquad \text{Equation 4.4}$$

Where:

F_B – Bouyancy force

ρ – Density of fluid

g – Gravitational acceleration

V – Volume of submerged body

3.3 Example of experiments to support the different understandings of buoyancy

There are different examples on experiments that support the piston school and the volumetric school. Both with their arguments and counter arguments.

3.3.1 An experiment favoring piston method of calculating buoyancy

Goins experiment:

Referring what Aadnøy says in his book[1]; "The common concept that buoyancy is equal to the weight of fluid displaced is true only sometimes". He is going further with this to explain what is happening with the piston force method, saying: "Buoyant forces exist only when there is an exposed end or cross-sectional area to which the hydrostatic pressure can be applied vertically".

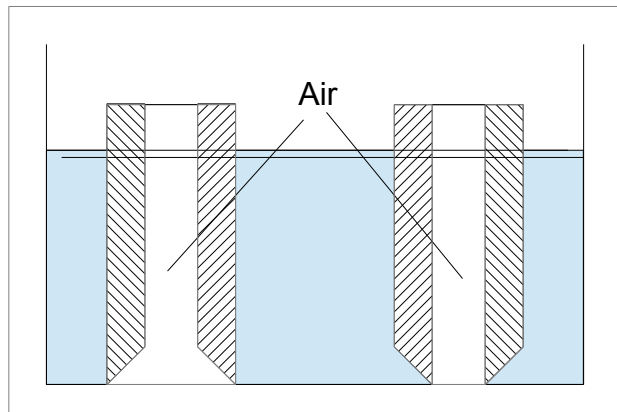


Fig 3-1: Goins experiment

Goins experiment contains a tank, with two cylinders with equal weight. One of the cylinders with an external bevel, the other one with an internal bevel, then the tank is filled with water.

A small experiment was conducted with plastic tubings. One cylinder with an external bevel, the other one with an internal bevel. The cylinders are equal in weight. A rubber mat was put on the bottom for proper seal between the bottom and the cylinders. Then water is filled in the bowl. None of the cylinders will float to the surface, but the cylinder with an external bevel tend to lift. Almost like the weight of the cylinder in water is gone, but barely not enough to lift off from the bottom. The cylinder with an internal bevel never tend to lift from the bottom. It stand firm on the bottom as if there was no water in the bowl.

The explanation to this phenomenon is said to be that the cylinder with an external bevel has an area where the vertical fluid pressure can act and lift the cylinder. The cylinder with internal bevel displaces more fluid, but is missing an area where the water pressure can act in a vertical direction.

Some people think this theory is wrong. By using the equations on effective tension from Sparks [5] and DNV, it is possible to find that the cylinders both are subjected to buoyancy [18] [25].

$$T_e = T_{tw} - P_i a_i + P_e A_e$$

Equation 4.5

Where:

$$P_i = 0$$

$$T_{tw} = -W$$

$$P_e = \rho g h$$

Then:

$$T_e = -W + \rho g h A_e$$

$$T_e = -\text{Weight} + \text{Bouyancy}$$

3.3.2 An experiment favoring Volumetric method of calculating buoyancy

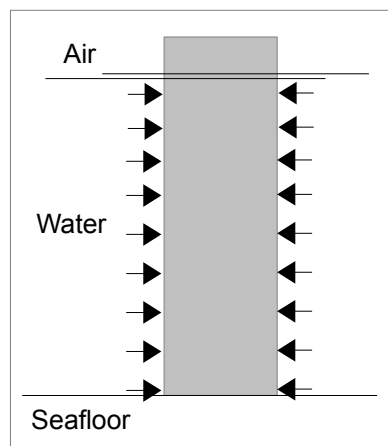


Fig 3-2: Cylinder on seafloor

Lets do an imaginary experiment. A cylinder barely lighter than water is glued to the bottom of a basin, there is no water or other hydrostatic pressure from underside. If basin was not filled, the cylinder will easily buckle. In the water, the cylinder will stand perpendicular to the bottom. It will also never buckle. This will mean there is no pressure difference over the vertical cylinder, but as the cylinder will never buckle, there is buoyancy force present. The pressure difference over the diameter is zero and there is no water pressure from underneath.

The piston method will get a higher compressive stress at the bottom compared to the volumetric method. The followers of piston method explain the buoyancy with a not perfect straight cylinder. The cylinder will fall to the side and go spiraling up towards lower pressure. The more equal densities between water and the cylinder, the more visible spiraling [26].

Piston method:

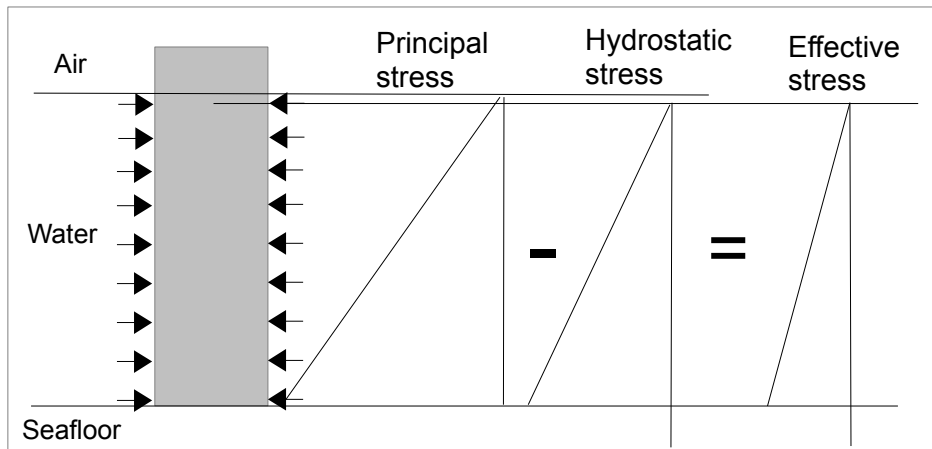


Fig 3-3: Cylinder on seafloor, piston method

Volumetric method:

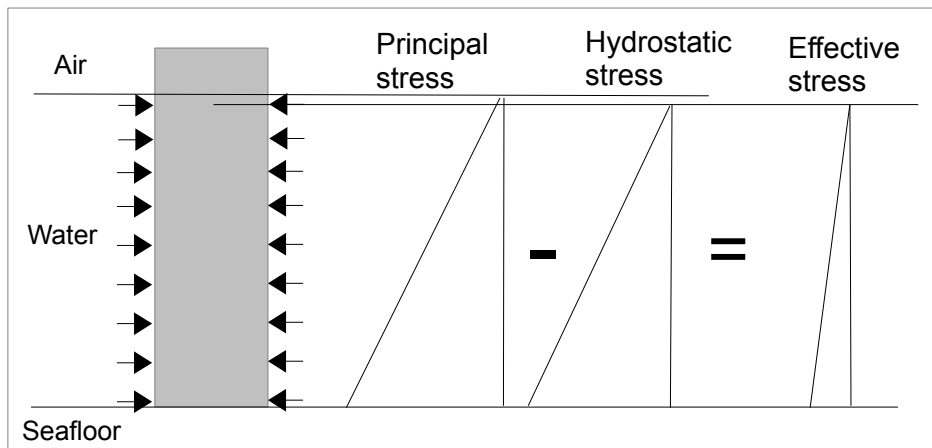


Fig 3-4: Cylinder on seafloor, volumetric method

- Principal stress:

All stresses acting on and in the body. Also called true stress.

- Hydrostatic stress:

Stress from the water on the body. This is equal to the pressure.

- Effective stress:

Stress used by the engineers for dimensioning. Also called deviatoric stress.

As seen the principal stress is lower for the volumetric method because of the buoyancy that will act in the axial direction and affect the principal stress so it will get smaller.

4. Body forces under hydrostatic load

It is possible to find the internal forces in submerged bodies by using super positioning.

4.1 Effective tension

The effective tension theory was explained in the book "Fundamentals of Marine Riser Mechanics " by Charles P. Sparks [5.]. He wanted to present the effective tension in risers in a more simple way as there are many people who struggle with understanding the effective tension concept.

4.1.1 Solid submerged body

Looking at the internal forces in a segment of a submerged body, then using superposition [5] [25].

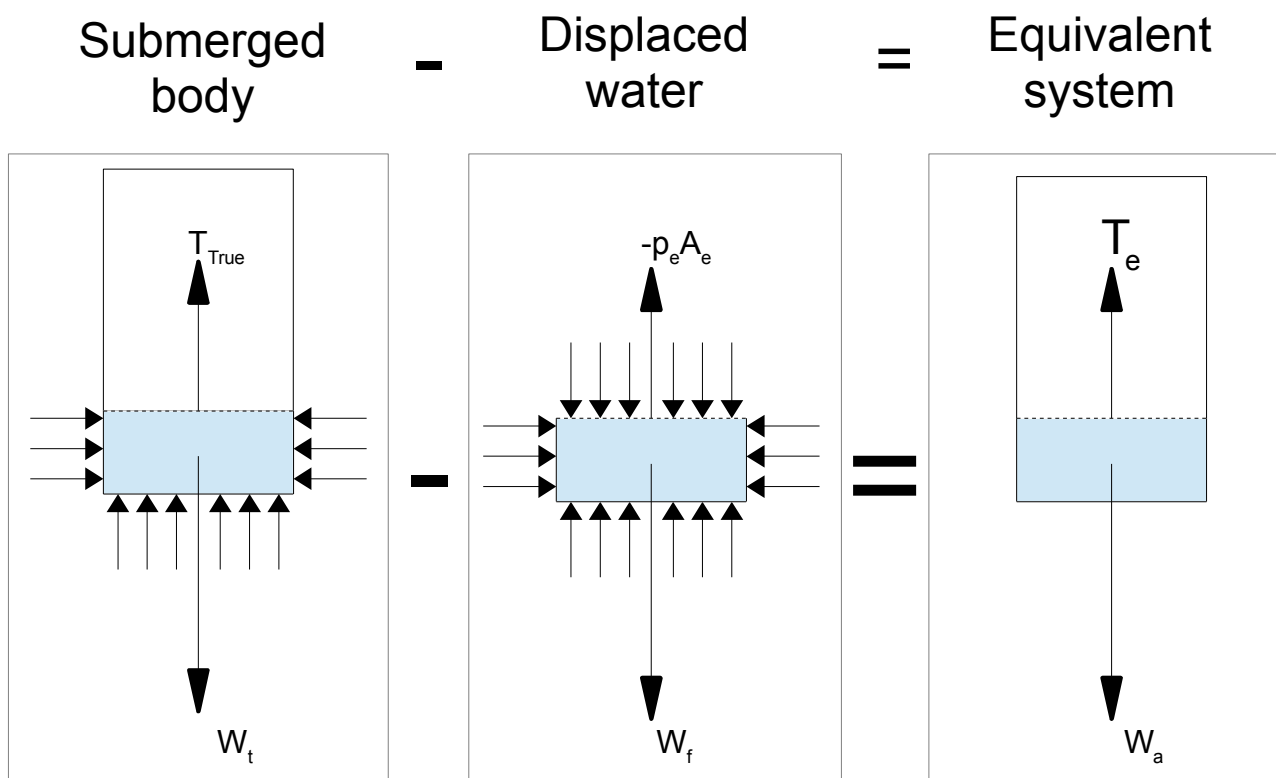


Fig 4-1: Effective stress in submerged solid body

$$T_e = T_{True} - (-p_e A_e)$$

Equation 5.1

$$T_e = T_{True} + p_e A_e$$

$$W_a = W_t - W_f$$

Equation 5.2

Where :

T_{True} = True tension

T_e = Effective tension

W_t = True weight

W_a = Apparent weight

W_f = Weight of fluid

True tension is the actual internal force possible to measure inside the body when submerged.

Effective tension is the deviatoric stress, the dimensioning stress in the body.

True weight is the weight of the body with no external forces, the weight of the body in vacuum.

Apparent weight is the weight of the body when exposed to external forces, the weight on a scale under water.

4.1.2 Pipes

A pipe is subjected to internal and external pressure. By adding the forces acting from the inside and subtracting the forces acting from the outside, the equivalent system remaining where all pressure effects are eliminated. Remaining forces are effective tension and the apparent weight.

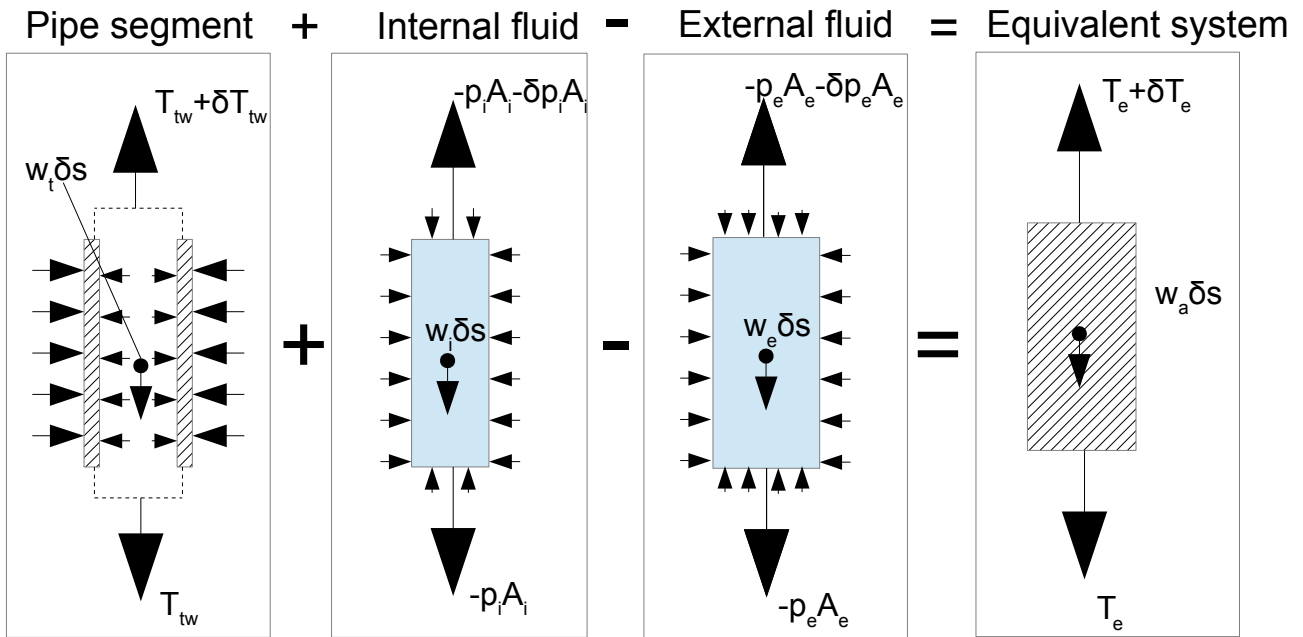


Fig 4-2: Effective stress in submerged pipe

$$T_e = T_{tw} + (-p_i A_i) - (-p_e A_e) \quad \text{Equation 5.3}$$

$$T_e = T_{tw} - p_i A_i + p_e A_e$$

$$W_a = W_t + W_i - W_e \quad \text{Equation 5.4}$$

Where T_e is the effective stress, T_{tw} is the principal stress with the internal pressure and external pressure as hydrostatic stress.

4.2 Effective stresses

Principal stresses can be split into effective and hydrostatic stress [9].

$$\sigma_p = \sigma_e + \sigma_h \quad \text{Equation 5.5}$$

There are only some very few and special materials that can fail due to hydrostatic stress, like soft rocks [2]. This is why engineers generally say that a material subjected to hydrostatic pressure only will not fail. Still, the material can change in volume. If weight is neglected, all stresses in a submerged body is hydrostatic stress. Hydrostatic stress is an equilibrium of stresses in all directions and exist even if water is not present.

Hydrostatic stress can be calculated as:

$$\sigma_h = \frac{\sigma_1 + \sigma_2 + \sigma_3}{3}$$

Equation 5.6

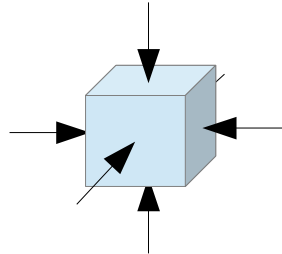


Fig 4-3: Stress cube

The stresses are measured relative to mean stress, known as effective stress. The mean stresses are pure tension or compression and shear stresses. The effective stresses are the stresses that is the dimensioning load for shear, tensile, compressive, buckling and collapse failures [2].

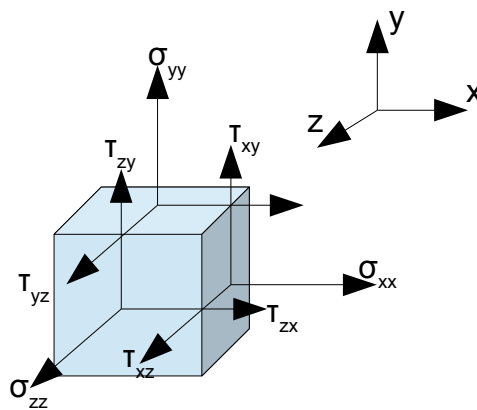


Fig 4-4: Stress and shear cube

effective stresses:

$$\begin{aligned}\sigma_{ex} &= \sigma_x - \sigma_h \\ \sigma_{ey} &= \sigma_y - \sigma_h \\ \sigma_{ez} &= \sigma_z - \sigma_h\end{aligned}$$

$$\sigma_e = \begin{bmatrix} \sigma_{ex} & \tau_{xy} & \tau_{xz} \\ \tau_{yx} & \sigma_{ey} & \tau_{yz} \\ \tau_{zx} & \tau_{zy} & \sigma_{ez} \end{bmatrix}$$

4.3 Tresca, Von Mises and Poisson

4.3.1 Tresca criterion

Also named the maximum shear stress criterion. It states that yielding will begin when the maximum shear stress at a point is equal to the stress at yield when subjected to uniaxial tension or compression.

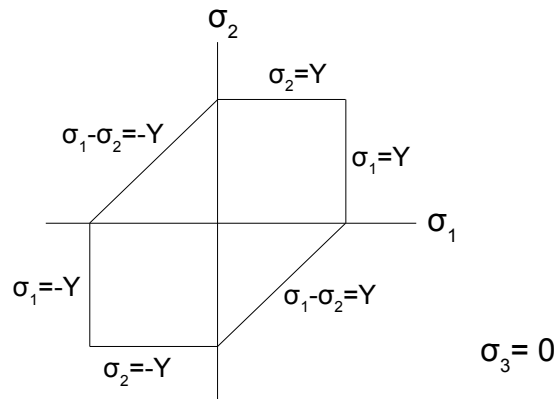


Fig 4-5: Tresca curve

For plastics, the yield strength in compression is often a lot higher than the yield strength in tension. Resulting in a non-symmetric yield curve.

For most situations the Tresca criterion agrees with experiments. For torsion however, the Tresca shear yield strength is conservative, approximately 15% higher than predicted [10]. The Tresca criterion is easier to apply than Von Mises criterion.

In 3 dimensions the Tresca and Von Mises yield surfaces will shape a hexagonal and a cylinder, both with direction:

$$\frac{1}{\sqrt{3}} \vec{i}, \frac{1}{\sqrt{3}} \vec{j}, \frac{1}{\sqrt{3}} \vec{k}$$

With hydrostatic axis as center where all principal stresses are the same. The deviatoric (effective) face or π -plane is angled 90 degrees on the hydrostatic axis. π -plane is the face where the sum of all the principal stresses are zero.

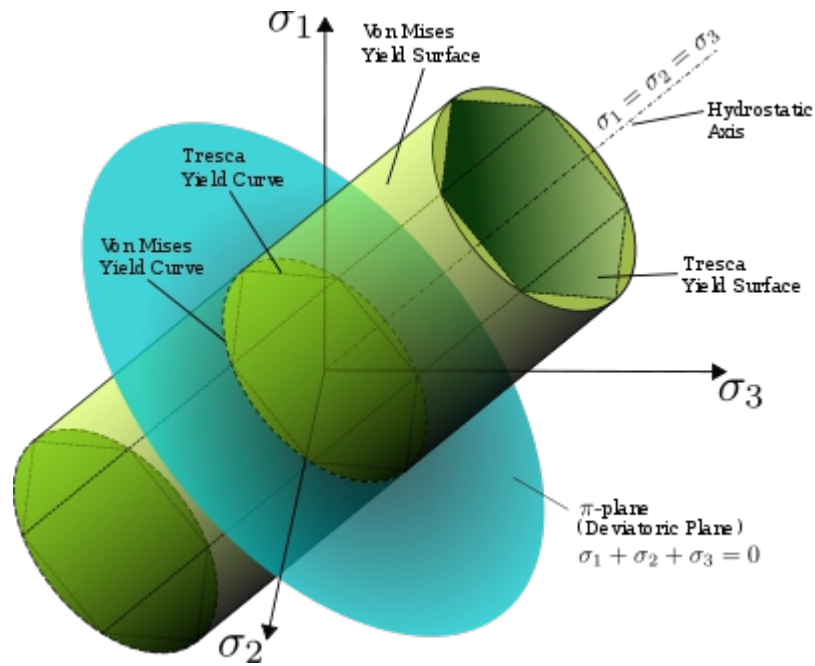


Fig 4-6: Tresca and Von Mises 3D curves

4.3.2 Von Mises criterion

The distortional energy density criterion (Von Mises stress criterion) states that "yielding begins when the distortional strain energy density at a point equals to the distortional strain energy density at yield in uniaxial stress" [10]. Meaning if the energy that is resulting in a volumetric change and shear in a body is too high, the element will fail. This way to look at stress will consider the volumetric change in the body. The hydrostatic stress is not considered.

The Von mises equation can be derived from strain energy density function:

$$U_0 = U_v + U_D = \frac{\sigma_1 + \sigma_2 + \sigma_3}{18K} + \frac{(\sigma_1 - \sigma_2)^2 + (\sigma_2 - \sigma_3)^2 + (\sigma_3 - \sigma_1)^2}{12G} \quad \text{Equation 5.7}$$

$$K = \frac{E}{3(1-2\nu)} \quad \text{Equation 5.8}$$

$$G = \frac{E}{2(1+\nu)} \quad \text{Equation 5.9}$$

At yield under uniaxial stress, $\sigma_1 = Y$, $\sigma_2 = \sigma_3 = 0$

$$U_D = \frac{(\sigma_1 - \sigma_2)^2 + (\sigma_2 - \sigma_3)^2 + (\sigma_3 - \sigma_1)^2}{12G} = \frac{2Y^2}{12G} = \frac{Y^2}{6G}$$

$$J_2 = -\frac{1}{6} [(\sigma_1 - \sigma_2)^2 + (\sigma_2 - \sigma_3)^2 + (\sigma_3 - \sigma_1)^2] \quad \text{Equation 5.10}$$

$$U_D = \frac{1}{2G} |J_2|$$

$$J_2 = I_2 - \frac{1}{3} I_1^2 \quad \text{Equation 5.11}$$

Where:

$$I_2 = \sigma_1 \cdot \sigma_2 + \sigma_2 \cdot \sigma_3 + \sigma_3 \cdot \sigma_1 = 0 \quad \text{Equation 5.12}$$

$$I_1 = \sigma_1 + \sigma_2 + \sigma_3 = \sigma = Y \quad \text{Equation 5.13}$$

$$\frac{1}{6} [(\sigma_1 - \sigma_2)^2 + (\sigma_2 - \sigma_3)^2 + (\sigma_3 - \sigma_1)^2] - \frac{1}{3} Y^2 = 0$$

$$Y = \sqrt{\frac{1}{2} [(\sigma_1 - \sigma_2)^2 + (\sigma_2 - \sigma_3)^2 + (\sigma_3 - \sigma_1)^2]}$$

Where:

U_0 = Total strain energy density

U_v = Volumetric change

U_D = Change due to distortion

U_0 = Total strain energy density

K = Bulk modulus

G = Shear modulus

I = Stress invariants

J = Deviatoric stress invariants

Y = Yield limit

4.3.3 Poisson ratio

Poisson ratio is a dimensionless ratio of the lateral strain that occurs in a body when the body is subjected to strain in the direction of loading. The ratio is from an uniaxial tension test. Most materials have a Poisson ratio between 0,25 and 0,33, plastics can have up to 0,47. [19]

$$\nu = \frac{\epsilon_l}{\epsilon_a}$$

Equation 5.14

Where :

ν = *Poisson ratio*

ϵ_l = *strain in non – loading direction*

ϵ_a = *strain in loading direction*

5. Fracture mechanics of plastic materials

Bridgman experiment was conducted with acrylic glass rods, a thermoplastic material. Thermoplastic materials have in common that yield loading strength is far lower than the failure loading strength. Also, the chemical bond inside the material is even stronger. The reason of the difference in strength between chemical bonds and failure is the small cracks and imperfections in the material. When a material is subjected to loading, these imperfections and cracks are growing until they reach a catastrophic size and the material will fail. We want to keep the material in compression to avoid propagation of these imperfections [24.].

5.1 Fracture mechanics

Bridgman did several experiments on tension and compression under hydrostatic stress. From the fractures, he found that hydrostatic stress affect the ductility of the materials. He could see that higher pressure gave smaller cross section area when specimens fractured in high pressure compared to low pressure. There were concluded that hydrostatic tension promotes formation and growth of voids, hydrostatic compression will suppress formation and growth of voids. In Bridgman experiments, the fracture was a necking down type, from full to low or zero cross sectional area.

A normal fracture that would be expected in thermoplastics, is grow of void nucleation at first, small pockets of empty holes in the material. The voids will grow as the forces are raising. Further development could be a brittle fracture between the voids, or the voids will grow together.

There are three main failure types in tension. Necking down, surface normal to axis and shear fracture [28]. What fracture type that will develop is depending on the material properties.

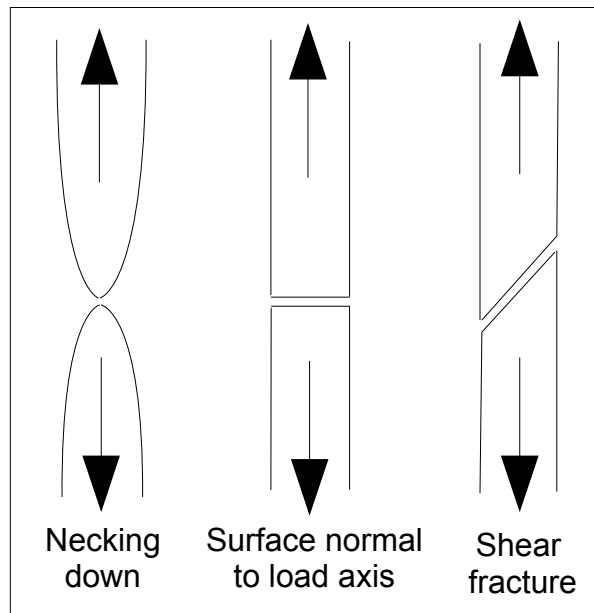


Fig 5-1: Tension failure types

All three of these fracture types are openings, there are two more fracture modes. Mode I; opening, mode II; shear in plane and mode III; shear out of plane.

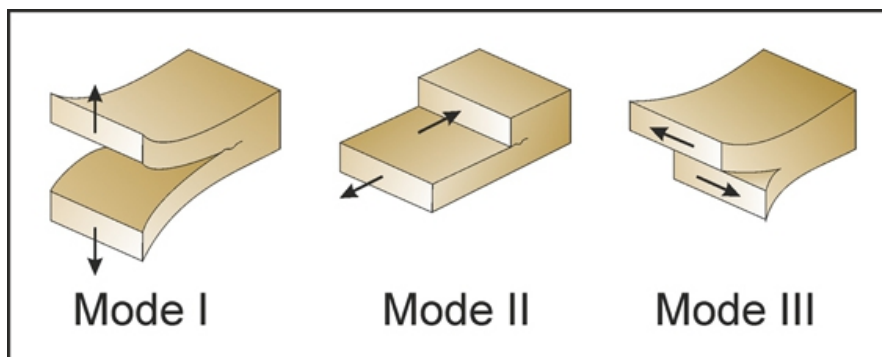


Fig: 5-2: Fracture types

In addition to the fracture types and modes, there are important fracture and material properties which will affect the fracture:

- Ductile or brittle, this is the material ability to deform. A ductile material like aluminum is easier to shape and bend than a brittle material like glass.
- Cleavage is a common fracture type in crystals where the body fracture along flat planar surfaces. The surface is determined by the structure of the crystal. Cleavages normally have reflective surfaces. [29.]

- Micro-void coalescences occurs due to nucleation of micro-voids. They will grow and join. The initiation of micro-voids are caused by stresses. On the fracture surface, they will look like parabolas and circles, depending on stress situation [30.].

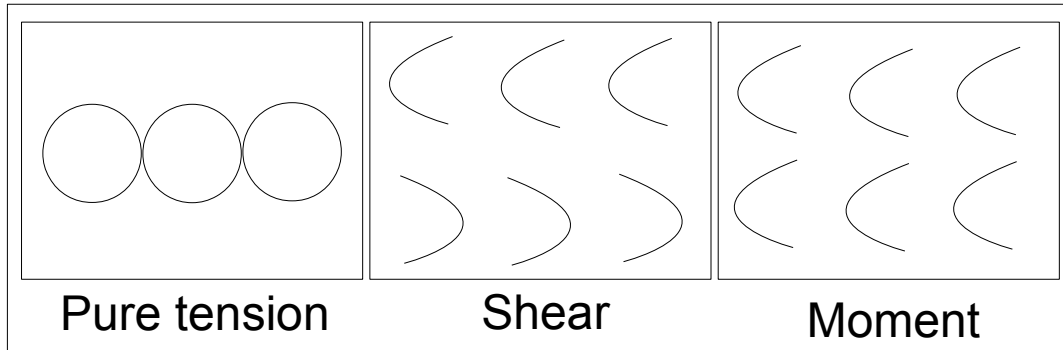
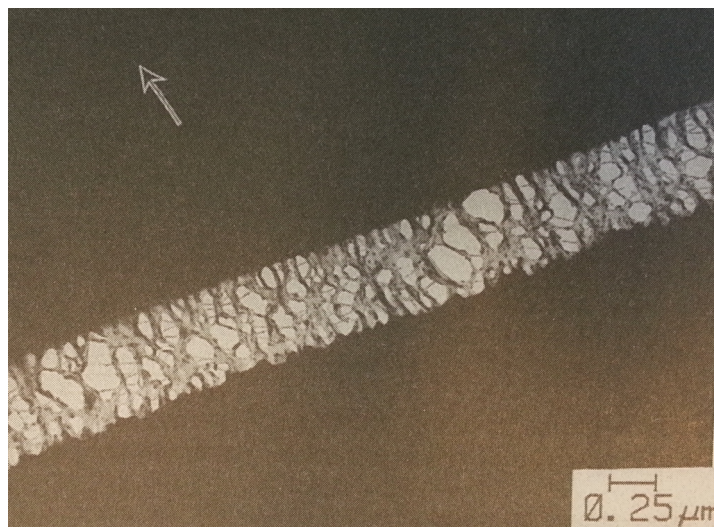


Fig 5-3: Void types

- Flank. A small cut. Often used to control fracture location.

- Crazeing is microscopic lines or gaps observable in glassy polymers. The gaps comes after a change in volume, as a response to tensional stress/strain in the material. They are developed from imperfections in the surface of the material and usually forms perpendicular to the maximum principal normal stress. A large hydrostatic tensile component in the stress tensor is conducive to crazeing [24]. Typical crazes has an intricate network of fibrils connecting the two surfaces. To increase, the crazes must either draw more material from the sides in the crack or develop into a fracture [7.] [27.].



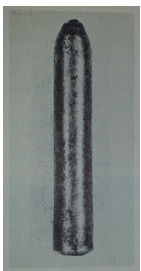
Pic 5-1: Crazeing, arrow is direction of loading

6. Looking at fracture surfaces from Bridgman experiment

6.1 Bridgman's fracture observations and fracture model alternatives

During the work on Bridgman experiment there has come up some interesting ideas on how the rod fractures.

6.1.1 Bridgman's observations



*Pic 6-1:
Pinch-off by
Bridgman*

Bridgman came up with these observations:

Mild steel/Copper/brass: Looks like a tensile break, but a bit more abrupt.

Harder materials as chrome nickel steel/vanadium steel: Irregular fracture, a combination of necking down and of a slip on shear planes at 45 degrees.

Glass hard tool-steel/glass/glass tubing: clean break with right angles and no necking.

Bridgman also explain that when ductile materials started necking, the axial tension force in the rod will raise. He further explains the tensile stress at the rupture as an incident and say the tension is not the true case of the rupture. He also see the rupture and the ultimate tensile stress coincide. The maximum stress criterion is applicable.

Bridgman put up three conditions for rupture. Maximum principal stress, maximum stress difference and maximum strain. Maximum principal stress is well known, tensile or compression. The second condition say that the difference between the greatest and least, exceeds a critical value. This is a criterion not far from Von Mises criterion. Third condition demands that fracture occurs when strain in any direction exceeds a critical value.

6.1.2 Fracture model alternatives

When the experts were interviewed, there were many different approaches to explain the fracture.

1. Material goes plastic under high pressure.

When Bridgman did his experiments, Kahlbaum, Roth claimed that materials might go into a plastic state or even fluid under high hydrostatic pressure. This is no longer a correct claim, Bridgman mentioned his experiment and the fact that some of his experiments were not valid as the pressurized fluid used by Kahlbaum became solid under the high pressure. Also, experiments show materials become more rigid under high pressure [12].

2. Piston force through cracks

Water is entering the rod through small cracks in the surface, creating pressure in rod which will act as a tension force in the fracture.

3. Poisson effect I

Packs in both side of the pressure vessel will create a situation were the rod is rigid in either end. Static friction is high. When the vessel is pressurized, the rod is experiencing a compressional axial force as a result of the Poisson ratio, where the rod want to squeeze in axial direction.

4. Poisson effect II

The rod will shrink in diameter and expand in length. This will create a fictitious tension force in the axial direction. When the strain and tension grows too big, the rod ruptures at Von Mises stress. This is the most popular explanation.

5. Effective tension

When rod is subjected to pressure on the curved surface, this equals to a tension force like the pressure times the cross sectional area. When pressure is high enough, the rod ruptures because of tension stress.

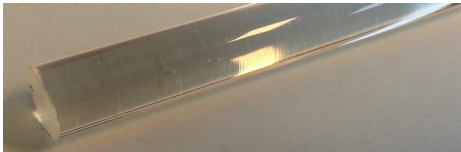

6.2 Introduction



The spring of 2013, Morten Reve did an experiment during his master thesis: "Bridgman experiment" on the pinch-off effect. Reve was working on "Understanding the buoyancy in drill pipes and risers". He was also looking at the forces and expected forces for the rods to fracture. This experiment will focus on the reason of the fracture and try to find the mechanism behind the fracture in the Bridgman experiment. The purpose of this work is to go further into the experiment, looking at different materials and other types of situations to find similarities by using new technology and knowledge to help explaining the experiment. Then it might be possible to see what is happening and find the mechanism behind the fracture of the rods.

Several experiments have been done to find differences or equalities between the fracture surfaces of the rods. All the rods went through the Bridgman experiment. Next, all the different types of rods were bent by hand to get a surface varying from tension to compression. Then, all the different types of rods were fractured by tension in a tension machine. After all experiments were conducted, the rods were cut down in size and put into the electron microscope for further analysis.

6.3 Materials

There are used four different rods:

Rod	Material and color	Picture
1	PMMA (acrylic glass) Color: clear Properties: not flexible, brittle.	 <i>Pic 6-2: PMMA</i>
2	POM-C Color: black Properties: flexible, ductile	 <i>Pic 6-3: POM-C</i>

3	POM-C Color: white Properties: flexible, ductile.	 <i>Pic 6-4: POM-C</i>
4	PA-6 Color: light gray Properties: very flexible, very ductile.	 <i>Pic 6-5: PA-6</i>

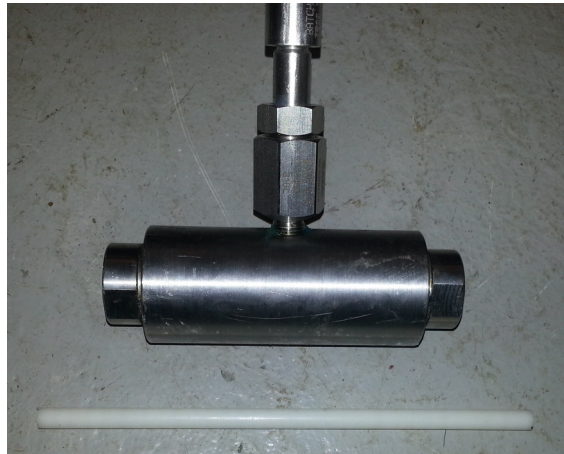
PMMA is an acrylic thermoplastic, well known as acrylic glass or Plexiglas. Its a brittle material, but does not shatter. It can be formed by heating. PMMA is often used instead of glass, its lighter and easier to work with. Often used where curved glass surfaces is needed. In this experiment, PMMA is used because its clear. Some lines were discovered in Reve`s master thesis, these lines will be further examined. [21.]. Pictures of the surface of the rod was taken and is shown in appendix F.

POM-C is an engineering thermoplastic because of its high strength, low friction and creep resistance. Mostly used by the petroleum and marine industry for rollers, washers, in bearings, for load support gears and pumps. POM was chosen for this experiment because it is more flexible than PMMA, hoping for a different fracture surface. [22.] [23.]

PA-6 is the most used engineering thermoplastic in Europe. Low friction, high strength. PA is used mostly as a lubricated wear and tear material, like in washers or gearing. PA will absorb water. PA was chosen for this experiment because it is very flexible. [23.]

6.4 Bridgman experiment

Bridgman experiment that is ending in the pinch-off effect, is done by setting a rod through a pressure vessel. In our case, the vessel length is 54 mm between the seals. When increasing pressure, the rod will fracture when the pressure is high enough.



Pic 6-6: Bridgman pressure vessel

The pressure vessel used in this experiment is seen above [Pic 6-5].

To fit the POM-C rods through the vessel, the rods were machined down to a bit below 8.1 mm in diameter.

The pressure vessel is connected to a high pressure unit. Inputs are water and air at pressure, output is high pressure water.

In the top left corner, there is an on/off valve for the pressure. Pressure is adjusted at the wheel down to the left. At top right, there is an adjustable valve for the pressure out. The bleed valve is located at the bottom right. The pressure gauge used is the big round display where the pressure at fracture was red off.



Pic 6-7: High pressure unit

6.4.1 Bridgman experiment results

Only three of the four rods went through the experiment, the PA-6 rod shrunk in diameter and elongated, it did not seal the vessel. This resulted in pressure drop to atmospheric pressure.

Tab 6-1: Bridgman experiment, pressure and material strenghts

Rod	Diameter Post test [mm]	Rupture pressure [bar]	Area post test [mm ²]
POMC black	7,84	950	48,3
POMC white	7,86	1000	48,5
PMMA	7,98	750	50,0
PA6	7,65	X	46,0

Tab 6-2: Bridgman experiment, diameter and lenghts

Rod	Length Pre test [mm]	Diameter Pre test [mm]	Length Post test [mm]	Diameter Post test [mm]
POMC black	198	8,05	201	7,84
POMC white	211	8,09	214	7,86
PMMA	207	7,98	207	7,98
PA6	202	8,1	207	7,65

Tab 6-3: Bridgman experiment, strain

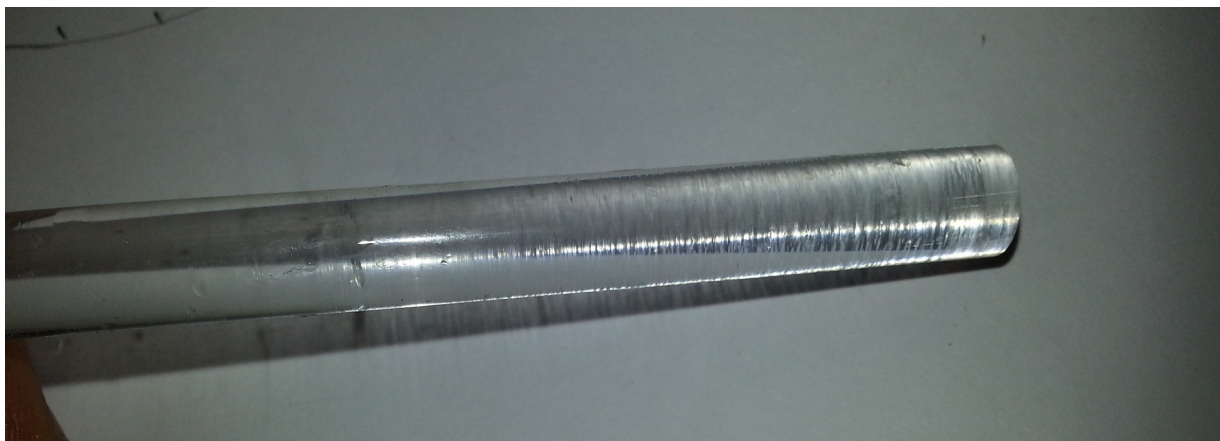
Rod	ΔL [mm]	L_0 [mm]	Strain $\Delta L/L_0$
POMC black	3	54	5,56%
POMC white	3	54	5,56%
PMMA	0	54	0,00%
PA6	5	54	9,26%

The PA-6 rod is significantly decreased in diameter. It is easy to see the spot where the diameter is smallest, this is also where the seal did not hold.



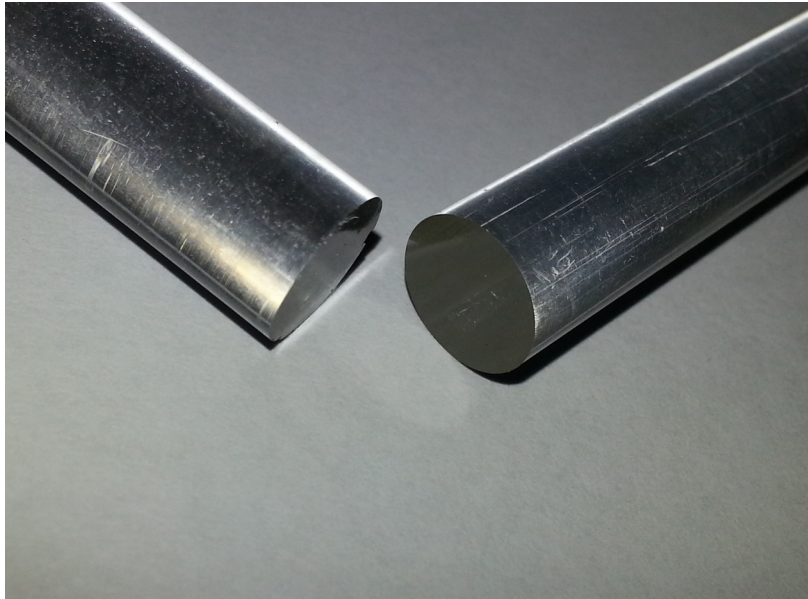
Pic 6-8: PA-6 rod fail

The PMMA rod had signs of crazing inside the pressure vessel. In the picture [Pic 6-8], the fracture surface is the cut at right, the crazing seems evenly distributed all the way from seal to seal in the pressure vessel. The crazes were also observed before the pressure was high enough to fracture the rod.



Pic 6-9: PMMA rod crazing

The PMMA rods had all a very smooth fracture surface.



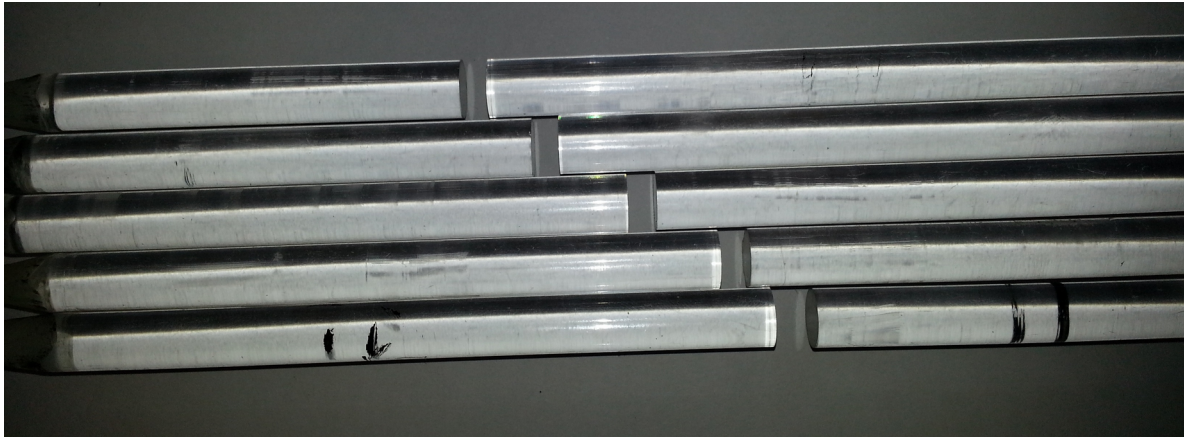
Pic 6-10: PMMA fracture surface

The POM-C rod had a right angled surface, with an edge across.



Pic 6-11: POM-C fracture surface

The fracture occurred at random location inside the chamber [Pic 6-12]:



Pic 6-12: Random fracture location

6.4.2 Bridgman experiment SEM results

Appendix A1: Bridgman experiment PMMA

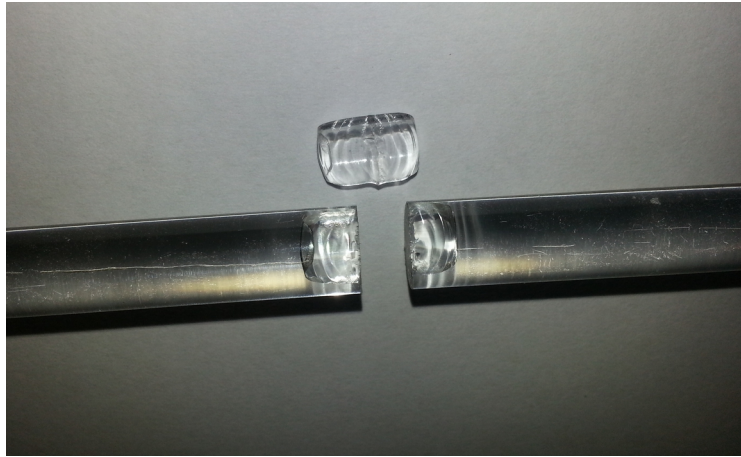
A smooth and reflective surface that did not come visible before it was put into the SEM (Scanning Electron Microscope). It looks like the fracture origin is at the right edge, where it is a light spot. Propagating to the left. The ridges along the left edge and the parabolas does support this.

Appendix A4: Bridgman experiment POM-C

The fracture surface of the rod subjected to hydrostatic forces in the pressure vessel has a smooth surface. There is an edge going across the surface that is probably a result of the machining when the rod was cut down in diameter. Closer images show the edge is more like a ductile fracture. The machining made a track on the curved surface where the fracture could follow and develop around the rod. Otherwise, the rod is evenly rough.

6.5 Bending experiment

All types of rods were bent by hand to make a fracture surface or at least a cross section with both tension and compression.



Pic 6-13: PMMA bending fracture



Pic 6-14: POM-C bending fracture

6.5.1 Bending experiment result

The PA-6 rod would not break without bending several times. Both PMMA and POM-C rods broke with a small fragment flying off on the pressure side of the cross section. As the rods will not fracture due to compression, the compression side will fracture due to in plane shear compared to the side subjected to tension which will create an opening. [24.]

6.5.2 Bending experiment SEM results

Appendix A2: Bending experiment PMMA

The bending experiment has similar characteristics in the top, the zone subjected to tension, where the fracture started. The fracture propagated further down. The parabolas with dark spots inside are showing directions of propagation of the fracture. Further down there are fewer and fewer dark spots and the parabolas goes over to be more like circular. The surface gets rough before the edge

abrupt with a missing fragment. Where the cross section was subjected to compression.

Appendix A5: Bending experiment POM-C

The rod subjected to bending has a smooth surface at the top at the fracture origin and developed quick. Further to the opposite side, it looks smooth and irregular. Then more and more rough before the edge abrupt the surface where a fragment broke off during the fracture.

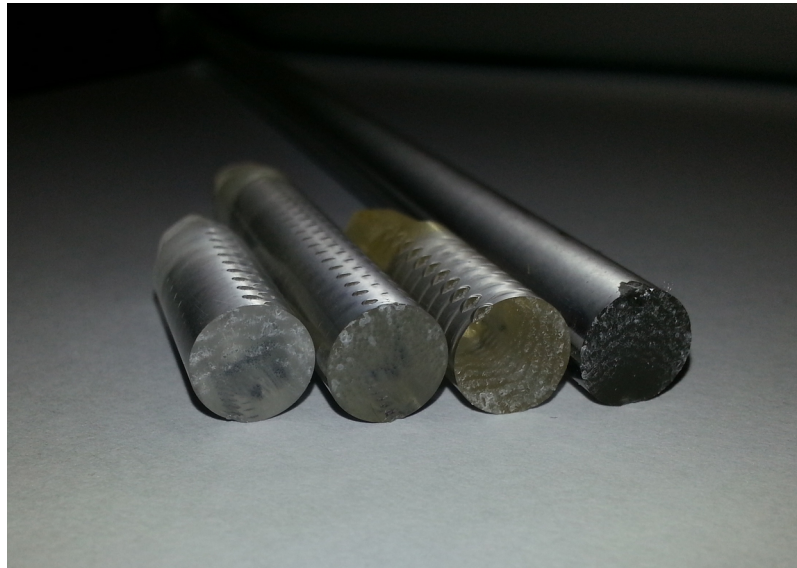
6.6 Tension loading experiment

All rods were loaded to fracture by using a tension machine. Before the rods were clamped in place, a flank were made in some of the rods to control the fracture location. Then tension were added. Force and strain was continuously measured by a computer during the deformation.



Pic 6-15: Tension machine

6.6.1 Tension loading experiment results



Pic 6-16: PMMA tension fracture

Three of the four different rods successfully went through the experiment, the PA-6 rod was too flexible and did not break in the tensile machine when no flank was made. The rod elongated and the test was stopped as the clamps was starting to loose their grip.

Tab 6-4: Tension experiment, load and material strenghts

Rod	Rupture load [N]	Diameter [mm]	Area [mm ²]	Material strenght [Mpa]
POMC black cut	2210	6,55	33,7	65,6
POMC black	3270	8,43	55,8	58,6
POMC white cut	2690	6,89	37,3	72,1
POMC white	3540	8,42	55,7	63,6
PMMA cut	2137	7,00	38,5	55,5
PMMA	2580	8,00	50,3	51,3
PA6 cut	1740	7,15	40,2	43,3
PA6	X	8,41	56	X

Reading the strain from the graph [Appendix E], rods with a flank is omitted:

Tab 6-5: Tension experiment, strain

Rod	Strain $\Delta L/L_0$
POMC black	5,80%
POMC white	5,50%
PMMA	1,80%
PA6	>25%

The values of PMMA is the average of the two tests conducted.

6.6.2 Tension loading experiment SEM results

Appendix A3: Tension loading PMMA

The fracture surface of the tension subjected rod is looking like something in between the one from the Bridgman experiment and the one which was subjected to bending. This fracture surface have a smooth spot to the upper right, where the fracture started. The same type of parables can be seen and further to the opposite side, the parables goes to be more circular and the surface gets more rough.

Appendix A6: Tension loading POM-C

The rod subjected to tension have a clear sign of an evenly rough surface, especially where the fracture started. At this spot in the top of the picture, the surface looks similar to the rod subjected to hydrostatic forces. It looks smooth and random further to the opposite side. Then more and more rough.

6.7 Discussion

6.7.1 Bridgman experiment discussion

When the PMMA rod fractured, there was no surprises, the experiment was done by Reve earlier and everything went as expected.

Crazing was observed in the PMMA rod, this is a sign of tension [27.] [7.]. Still, there was no measurable difference in length of the rod. Reason could be that the length different is small, or that the rod is expanding and retracting again just after the fracture. This could also be the reason to why the crazing will disappear or be invisible after 15 - 30 minutes. Another explanation could be that water go into the crazes to make them visible and later is absorbed or squeezed out before it is evaporating. In Appendix A1 there is a color variation from light to dark when looking from the outside edge, this is where the crazes are suspected to end. Water could enter the crazes and create an additional force that will generate a fracture surface like tension. When the pressure is high enough, fracture will rapidly increase through the whole cross section.

If the rod was fractured because of pure tension, the material strength could be calculated with use

of effective tension theory:

Tab 6-6: Bridgman tension material strength, volumetric

Rod	Diameter Post test [mm]	Rupture pressure [bar]	Area post test [mm ²]	Strength [N]	Friction [N]	Rod Strength [N]	Material Strength [Mpa]
POMC black	7,84	950	48,3	4586	450	4136	85,68
POMC white	7,86	1000	48,5	4852	450	4402	90,73
PMMA	7,98	750	50,0	3751	270	3481	69,60
PA6	7,65	X	46,0	X	X	X	X

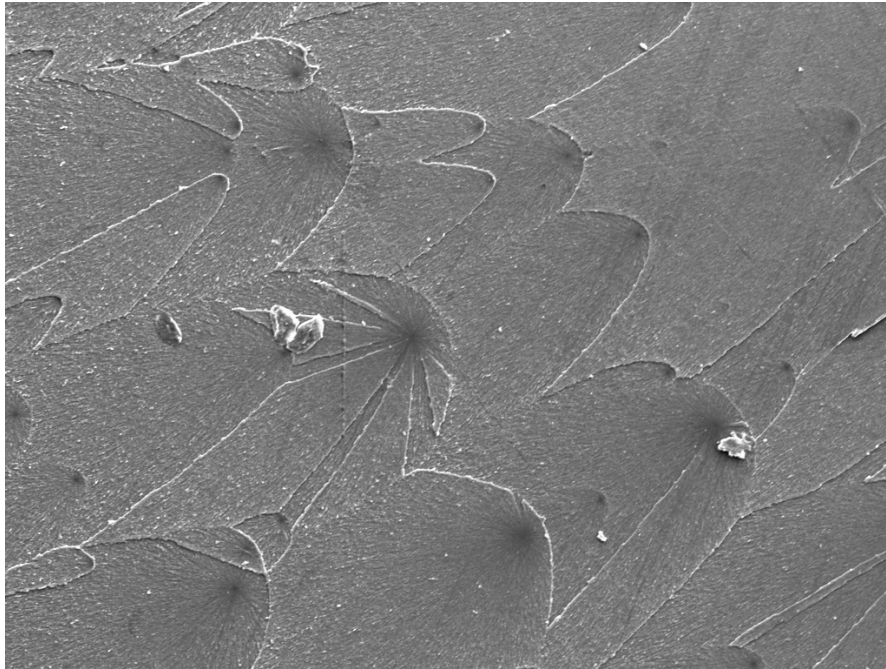
When tension is calculated with use of Poisson ratio and pressure [See 2.1], material strength will be:

Tab 6-7: Bridgman tension material strength, piston

Rod	Diameter Post test [mm]	Rupture Pressure [bar]	Area post test [mm ²]	Poisson ratio	Rod Strength [MPa]	Friction [N]	Friction [N/mm ²]	Material Strength [Mpa]
POMC black	7,84	950	48,3	0,35	66,5	450	9,3	57,2
POMC white	7,86	1000	48,5	0,35	70,0	450	9,3	60,7
PMMA	7,98	750	50,0	0,38	57,0	270	5,4	51,6
PA6	7,65	X	46,0	0,39	X	X	X	X

Friction forces are red from graph [13]. Poisson ratios from the material property paper [32.].

The observations also support tension loading. As the fracture surface is perpendicular to the longitudinal axis of the rod and very reflective surface, not how a surface of shear fracture would look like. SEM photos will again support tension in the way voids grow and join.



Pic 6-17: Voids

When the POM-C rods were going into the pressure vessel, there were some challenges, instead of 8mm diameter, the rods were 8,4mm in diameter. Rods were sanded down to 8mm by using a drill and rough sand paper, then heated with a gas burner to get a smoother surface. When the experiment was conducted, it could look like the fracture surface was strongly influenced by the grooves from the sandpaper on the external surface of the rod. Fracture surface also became smoother along the edge where the sand paper was making a groove around on the surface of the rod.

The solution was to machine the rods to decrease diameter. After machining, there were still grooves on the surface of the rod, but the fracture surface changed significantly.

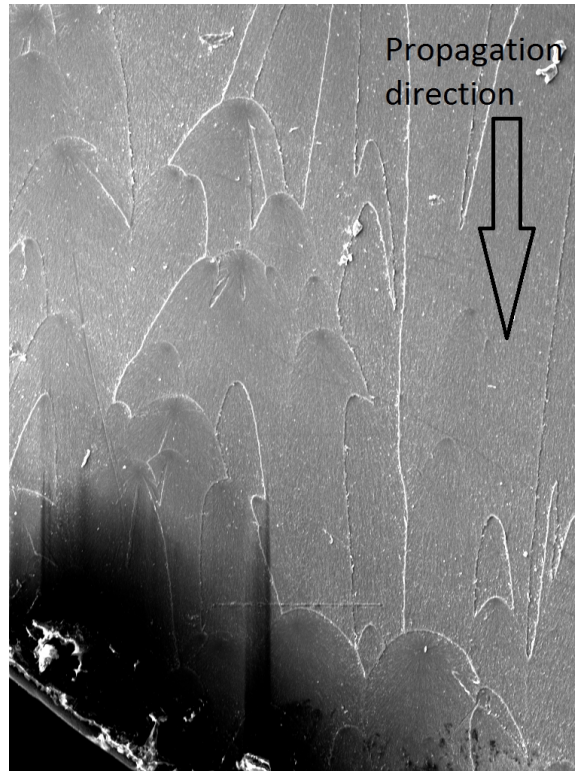


Pic 6-18: POM-C fracture surfaces. Sanded(l) and machined(r)

Again, the fracture surface is perpendicular to the longitudinal axis of the rod, indicating a fracture surface from tension.

6.7.2 Bending experiment discussion

This test was conducted to see the difference between compression and tension in the fracture surface. Also how the materials behaved under the different loadings. Then have a closer look at the fracture surface to distinguish pressure from tension.



Pic 6-19: PMMA fracture propagation

When fracture surfaces were photographed in SEM, the voids in PMMA confirm the directions of the fracture. The voids developed in radial direction from the small dark spots. When moment is present, the voids will tend to grow away from the opening as the two surfaces in the fracture are separating. [Pic 6-17]. The voids that developed into circular patterns, are from zones subjected to pure tension. The voids developed into parabolas, are from zones subjected to moments in addition to tension [27.].

6.7.3 Tension experiment discussion

This experiment was conducted to compare the fracture surface in pure tension to the fracture surface in the Bridgman experiment. The strain is red from the graphs [Appendix E] and is matching the strain from the Bridgman experiment well at around 5,5-5,8% in the tension experiment and 5,6% in the Bridgman experiment. All the numbers from rods with a flank was omitted due to the stress concentration which will affect the strength of the material. The PMMA rod has only 1.8% strain, which is a small deformation before break. Also, the graphs [Appendix E] does not say anything about how the rods are acting after the tensioning. Rods might retract.

The fracture surfaces in the POM-C rods are looking random and messy. There are tendencies of lines or ridges from one side of the fracture to the other. Some of the fractures also have a smooth surface at origin, with a clear limit where the fracture goes over to look random and messy.

6.8 Experiment summation

There are quite large variations of fracture load between the experiments. If the theory of effective tension is used to calculate the tension stress in the rods, result is:

Tab 6-8: Bridgman vs. tension material strenghts, volumetric

	POMC [MPa]	PMMA [MPa]
Bridgman experiment	86-91	70
Tension experiment	64-69	51

This clearly show that tension forces in the rods in Bridgman experiment have a trend to be higher than in tension. Reason might be that friction forces from the seal is higher than expected, or the stress should be calculated by the use of Poisson ratio in addition to the pressure as suggested in chapter 2.1. If the stress is calculated with the use of Poisson ratio, results are:

Tab 6-9: Bridgman vs. tension material strenghts, piston

	POMC [MPa]	PMMA [MPa]
Bridgman experiment	57-61	52
Tension experiment	64-69	51

When it comes to the observations of the fracture of the rods, it can be seen that all these tree rods, fractured in different ways, have similarities that are of the same kind of forces. All fractures are opening fractures and are perpendicular to the longitudinal axis. Pictures show the same type of voids in PMMA and structures like river markings from origin to end of the fracture in POMC.

Also the POMC rods have similarities that indicate the same type of force. There are differences in roughness and origin of the fractures, but they seem to be random or explainable by other mechanisms.

Both rods that fractured during the hydrostatic test have smoother surfaces (if the ridge in POMC is neglected) than the other tests. This might be explained by the speed of the fracture, how quick the rods went from one to two parts. The high pressure in the vessel will push the ruptured rod in

opposite ways. In the tension test, the rods will not move more than they are stretched, as soon as the fracture has started, the tension which is driving the elongation is rapidly decreasing. The fracture propagates slower to the opposite side. The slowest fracture is from the bending experiment, where the fracture speed is starting quickly with a snap and decreasing rapidly to the other side. This could explain the differences in roughness from start to end of the fracture in all the tests, and the difference in roughness between them.

6.9 Comments to experiments

Rod sizes:

The difficulties of getting hold on proper rods with a diameter that would fit in the pressure vessel made this experiment harder than expected. More tests of different materials could end up in another conclusion. Bridgman wrote that the stress to produce rupture always exceeded the tensile strength by 25-50%, except for glass. [12]. Also smoother machining or other treatment of the rods should be done to raise the quality of the fractures.

Use strain gages:

A rod with built in wire strain gage could measure the strain in the rod as the pressure is raising in the pressure vessel in Bridgman experiment. This would confirm if there are axial strain in the rod as soon as there are pressure acting on the curved surface and the relation between pressure and strain could be measured.

More rods of different, well known materials.

These experiments were focusing on the fracture surfaces, not numbers. By testing more rods and different materials, like metals, it might be possible to get some better results on how the fracture can be predicted and see similarities among more of the same rods subjected to the same forces to see the variety. If there are used more known materials, the results might be easier to analyze.

Faster ruptures.

Speed up the tension machine to create a rupture that is faster. This might be more equal to the fracture surface in the Bridgman experiment. Snap loads might also trigger a smoother surface.

Better readings.

It is hard to read off a pressure when the rod is fracturing so suddenly. A better gauge that can measure the maximum achieved pressure would help getting better numbers.

Closer look at crazing

Bridgman experiment could be stopped after half the pressure of rupture pressure, or at the stage when crazes started to form. Then take the rods to the SEM for inspection. This could give new information about how the crazes appear and at what pressure.

7. The software paradox

Reve put up a model of Bridgman experiment in OpenFOAM in his masters thesis. There were no sign of axial forces in the model that could lead to a fracture.

This is why Bridgman experiment was modeled in two more softwares to see if there are any differences between them. When the model was simulated the experts on the softwares were contacted to explain the results. The experiments show fracture surfaces as from tension fractures, a tension force is expected in the results.

7.1 Ansys

The tree step paradox was modeled in Ansys by John Normann Gundersen.

Appendix B1: Positive pressure on the inside of the pressure vessel.

Appendix B2: Positive pressure on the outside of the pressure vessel.

Appendix B3: Negative pressure outside the pressure vessel.

Then sending a mail to Ansys explaining the result and asking about why there is no axial tension stress in the rod when rod is subjected to hydrostatic stress on the curved surface inside the pressure vessel.

Ansys answered that their program will give a realistic result. The Bridgman paradox will give the same but opposite deformation and axial loadings with negative and positive pressures. Inner pressure will not give any axial stress. Any changes arrive from Poisson effects.

7.2 Autodesk Inventor

The problem was modeled in Autodesk Inventor.

Appendix C1: Positive pressure on the inside of the pressure vessel

Von Mises stress: Appendix C1.1: High and uniform in all the inside of the pressure vessel.

1st principal stress: Appendix C1.2: Small and uniform in all the inside of the pressure vessel.

3rd principal stress: Appendix C1.3: As expected. Radial stress is equal to the pressure.

Appendix C2: Positive pressure on the outside of the pressure vessel.

In the drawings, the rod is supported in the middle. Rigidly clamped. This should not affect the stresses that are important to the experiment as the problem is symmetrical. Any stress variation around this point is negligible.

Von Mises stress: Appendix C2.1: Uniform and high, equal to the inside pressure case. Only inside pressure vessel.

1st principal stress: Appendix C2.2: Small and compressive inside pressure vessel.

3rd principal stress: Appendix C2.3: High compressive stress.

Appendix C3: Negative pressure outside the pressure vessel.

Von Mises stress: Appendix C3.1: Uniform and high, equal to the inside pressure case. Von Mises stress is high only inside pressure vessel.

1st principal stress: Appendix C3.2: High tension stress as expected.

3rd principal stress: Appendix C3.3: Low tension stress inside pressure vessel.

Problem was posted on Autodesk community forums. The participants agreed there is no axial force from the pressure. The replies from the experts on Inventor agreed to the answers from Ansys. There is no axial force when pressure is acting on the curved surface. Reason for breaking is due to a Poisson effect, the necking down portion of the rod see tension. The necking down is also the only way the internal pressure directly can produce tension.

7.3 OpenFOAM

The Bridgman experiment was modeled in OpenFOAM by Bjørn Hjertager.

In the pictures, the inside of the pressure vessel is on the left side.

Appendix D1: Stresses in X direction

Appendix D2: Stresses in Y direction

Appendix D3: Stresses in Z direction

Appendix D4: Von Mises stress

Result is similar to the result of other softwares. No axial stress.

After several attempts, it has not been possible to get in contact with the OpenFOAM community experts to have their opinion.

OpenFOAM is an open software, anyone can open and modify the source code. This is often done in community as a cooperative work. There is not a single team or person who has written the program.

8. Results summarized

The results from the experiments were not very conclusive and does not clearly say which school is right. There are still major differences between the two schools that can not be solved. Still, there are similarities. Both schools agree the expected fracture will happen at a pressure. The pressure is calculated differently, but the result is the same. Also, both schools agree that the fracture surface will look like a tension fracture, again with different explanations on why. Below, there are listed some of the arguments which is favoring the two main schools.

School I: Compression (Poisson and Von Mises criterion):

- + Mathematic proofs, radial pressure does not make axial stress.
- + Fracture at expected pressure, Von Mises yield criterion.
- + Softwares are consistent.
- + Broad acceptance among experts.
- No grooves where pressure can create axial piston force

School II: Tension (Effective tension theory):

- + Easy and logic solution.
- + Good explanation on crazing and angle of fracture surface
- + Strain is equal to strain in tension experiment.
- + Fracture surfaces are like fracture surfaces from tension.
- Pressure is higher than expected.

9. Summation and conclusion

When Bridgman experiment was conducted, it was found that:

- The rod fractured at a pressure that is approximately 75% of the material ultimate tensile stress.
- The fracture surface is perpendicular to the longitudinal axis.
- Cracks on the surface of the PMMA rod, named crazes, appeared before fracture. For crazes to appear, the rod has to elongate.

In the bending experiment, there were observed tension and compression zones.

- The fracture surface on the tension side is perpendicular to the longitudinal axis of the rod.
- The fracture surface on the compression side is irregular and very different from everything seen earlier.

The tension experiment verified the results from both experiments above.

- The fracture surface is perpendicular to the longitudinal axis.
- The tension surface is similar to the fracture surfaces in both the Bridgman experiment and the tension side in the bending experiment.
- The strain measured in the tension experiment compared to the strain measured in the Bridgman experiment is equal.

The experiments conducted clearly show that the fracture surfaces from Bridgman experiments are surfaces looking the same as surfaces from tension fractures. However, this does not mean that there are tension stress in the rods at ultimate tensile stress. The reason of fracture could be a result of multiple mechanisms.

The PMMA rod seemed to have the most interesting fracture reactions like crazing and voids. Crazes perpendicular to the longitudinal axis of the rod appear before the fracture occur. They appeared even if there is no grooves in the surface from before.

The question is more on how the crazes appeared on the outside of the rod. No significant irregularities were found on the surface perpendicular to the axial direction [Appendix F]. The most significant lines on the outside surface were found in the axial direction, but does not seem to be of any interest. This indicates that there is an axial tension force acting in the rod before the crazes appear and that this tension force is sufficiently strong to create crazes on the surface. A tension force that could be explained by using effective tension theory as introduced by Charles P. Sparks. This theory is a new method aimed at calculating the effective tension in risers. In Bridgman paradox, the effective tension can be calculated by multiplying pressure and the cross sectional area of the rod.

The POM-C rod also have signs of different fracture mechanisms. In Appendix A5 there are seen a different and less irregular fracture surface at the origin of the fracture, compared to the rest of the fracture surface. Still, there is not observed other reactions in the rod that can imply the source of the fracture.

When the problem was modeled in the three softwares; Autodesk Inventor, Ansys and OpenFOAM, the results were similar. The axial stresses were negligible and Von Mises stress was at ultimate stress, equal to the pressure. When experts were contacted, both experts from Ansys and Inventor agreed. There should not be any axial forces and the only changes is due to Poisson effects. Several attempts were done, but no reply was received from OpenFOAM.

A number of experts have been interviewed and there are large variations in the explanations on the reason of fracture, but the explanations can still be placed in two schools. The ones that believe Von Mises criterion, Poisson effects and pressure on a curved surface is the dimensioning loads and the ones that believe the effective tension will give the dimensioning load.

References

[1].

Bertin, J.J. (c1987) *Engineering fluid mechanics / John J. Bertin*. Englewood Cliffs, N.J. : Prentice-Hall.

[2].

Aadnøy, B.S. and Kaarstad, E. (2011). *Theory and Application of Buoyancy in Wells*. Modern Applied Science. 5(3).

[3].

Fyrileiv, Olav and Collberg, Leif. (2005). Influence of pressure in pipeline design – Effective axial force. Det Norske Veritas. 24th International Conference on Offshore Mechanics and Arctic Engineering.

[4].

Aadnøy, B.S. (2006) *Mechanics of drilling / Bernt S. Aadnøy*. Aachen : Shaker Verlag.

[5].

Sparks, C.P. (c2007) *Fundamentals of marine riser mechanics : basic principles and simplified analyses / Charles P. Sparks*. Tulsa, Okla. : PennWell.

[6] <http://en.wikipedia.org/wiki/Crazing> (24.04.14)

[7] Buckley, C.P. Bucknall, C.B. Og McCrum, N.G. (1997) *Principles of polymer engineering / N.G. McCrum, C.P. Buckley, C.B. Bucknall*. Oxford : Oxford University Press.

[8].

Fenner, R.T. (1986) *Engineering elasticity : application of numerical and analytical techniques / R. T. Fenner*. Chichester : Ellis Horwood.

[9].

Jargon, F.E. (2005). *Hydrostatic and Deviatoric Stresses/PADT. The Focus*.

[10].

Boresi, A.P. og Schmidt, R.J. (c2003) *Advanced mechanics of materials / Arthur P. Boresi, Richard J. Schmidt*. New York : Wiley.

[11].

http://www.efunda.com/formulae/solid_mechanics/mat_mechanics/plane_stress_principal.cfm

(06.02.14)

[12].

Bridgman, P.W. (1964) *Collected experimental papers Volume 1/ P.W. Bridgman*. Cambridge, Mass. : Harvard University Press.

[13].

Morten Reve. (2013). Understanding of Bouyancy in Drillpipe and Risers. UIS, Masters Thesis.

[14.]

http://serc.carleton.edu/research_education/geochemsheets/techniques/SEM.html (23.04.14)

[15.]

Aadnøy, B. S. Bouyancy in petroleum engineering, Part 2: Applications. UIS, Presentation.

(08.05.14)

[16.]

<http://en.wikipedia.org/wiki/Buoyancy> (25.04.14)

[17.]

<http://src.gov.jm/wp-content/uploads/2012/12/buoyancy.pdf> (14.05.14)

[18.]

Nergaard, A. Is this where Goins went wrong. UiS (2011)

[19.]

http://www.instron.us/wa/solutions/ASTM_D638_Tensile_Testing_Plastics_Poissons_Ratio.aspx (26.05.14)

[20.]

<http://web.mit.edu/13.012/www/handouts/Reading3.pdf> (29.05.14)

[21.]

[http://en.wikipedia.org/wiki/Poly\(methyl_methacrylate\)](http://en.wikipedia.org/wiki/Poly(methyl_methacrylate)) (29.05.14)

[22.]

http://www.nylacast.com/semi-finished-product/pom-c-copolymer#.U4cSBfl_srU (29.05.14)

[23.]

<http://www.vink.no/nb-NO/Bruksomr%C3%A5de/Industri/Standard-teknisk-plast.aspx> (29.05.14)

[24.]

T. L. Anderson. (2005). *Fracture Mechanics, Fundamentals and Applications*. Boca Raton, FL. Taylor & Francis Group.

[25.]

Det Norske veritas. (2010) *Dynamic risers : offshore standard DNV-OS-F201 / Det norske veritas*. Høvik : DNV.

[26.]

Emails from Per Amund Amundsen (UiS) (15.05.14)

[27.]

Emails from Anne Serine Ognedal (NTNU) (29.04.14)

[28.]

Hosford, W.F. (2010) *Solid mechanics / William Hosford*. Cambridge : Cambridge University Press.

[29.]

http://flexiblelearning.auckland.ac.nz/rocks_minerals/minerals/fracture.html (31.05.14)

[30.]

[http://www.engineering-dictionary.org/Materials-Science-and-Engineering-Dictionary/microvoid_coalescence_\(MVC\)](http://www.engineering-dictionary.org/Materials-Science-and-Engineering-Dictionary/microvoid_coalescence_(MVC)) (31.05.14)

[31.]

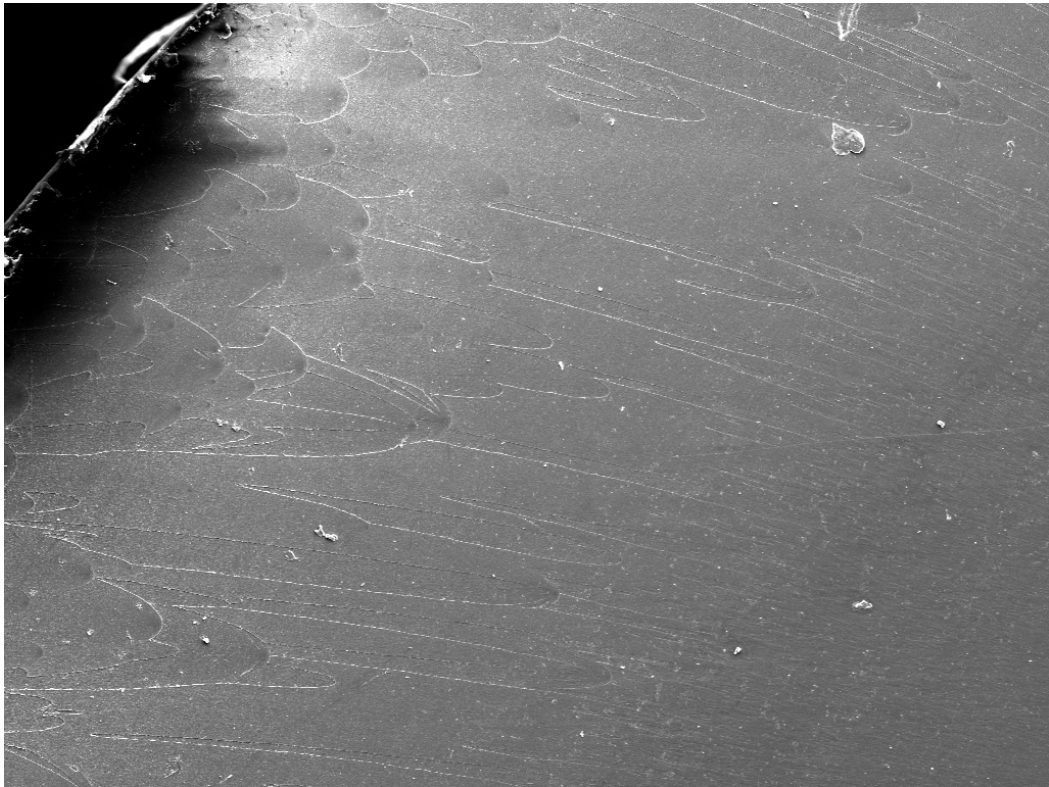
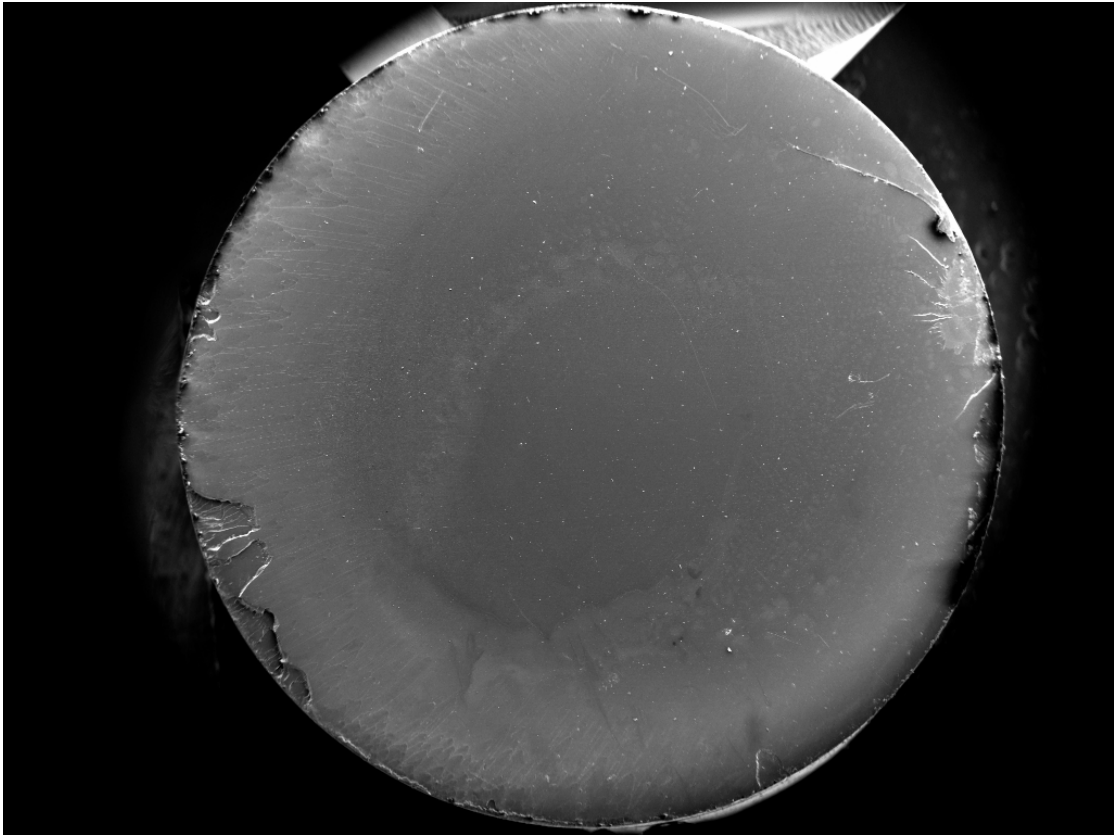
In conversation with Aadnøy, Bernt (UiS)

[32.]

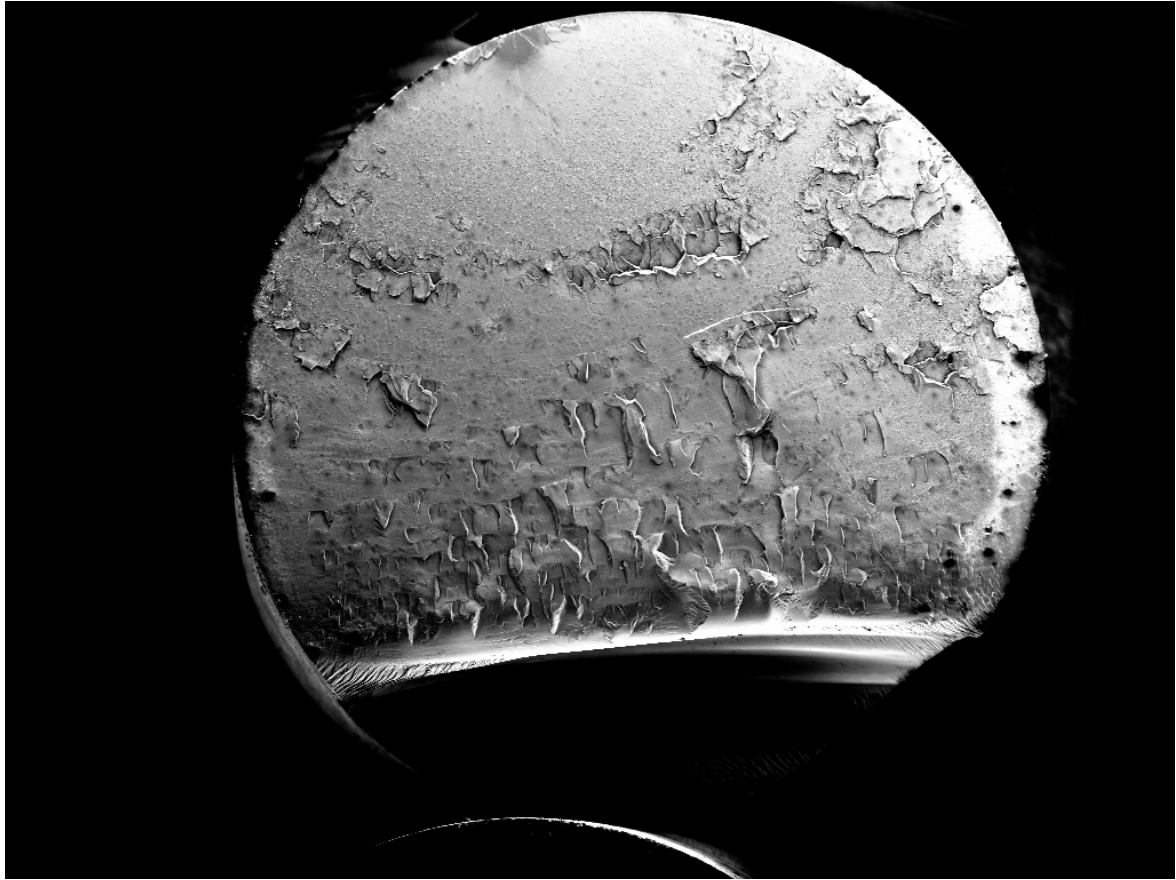
<http://www.goodfellow.com/E/Polyamide-Nylon-6.html> (05.06.14)

..

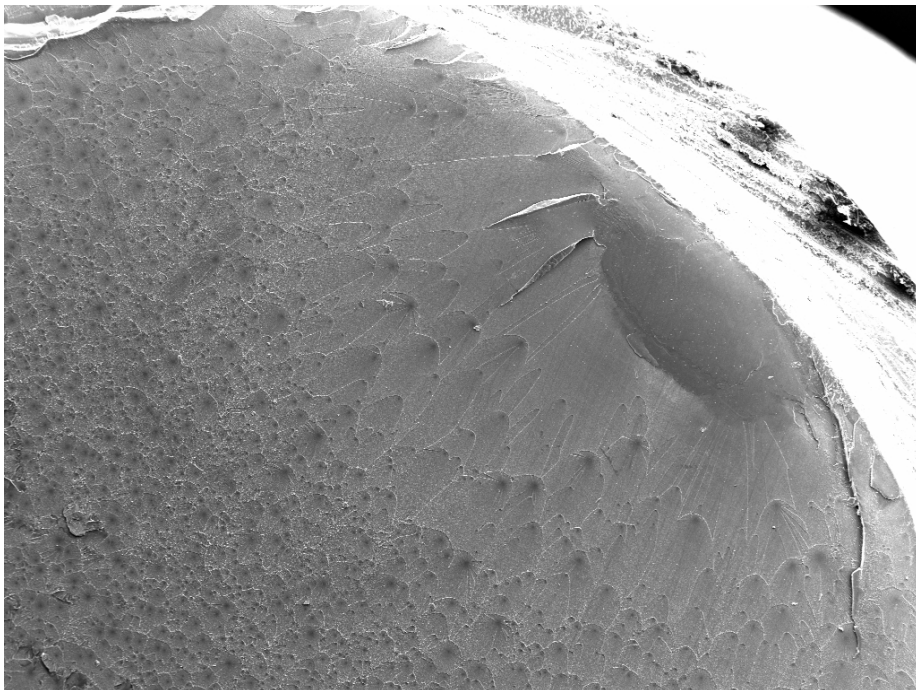
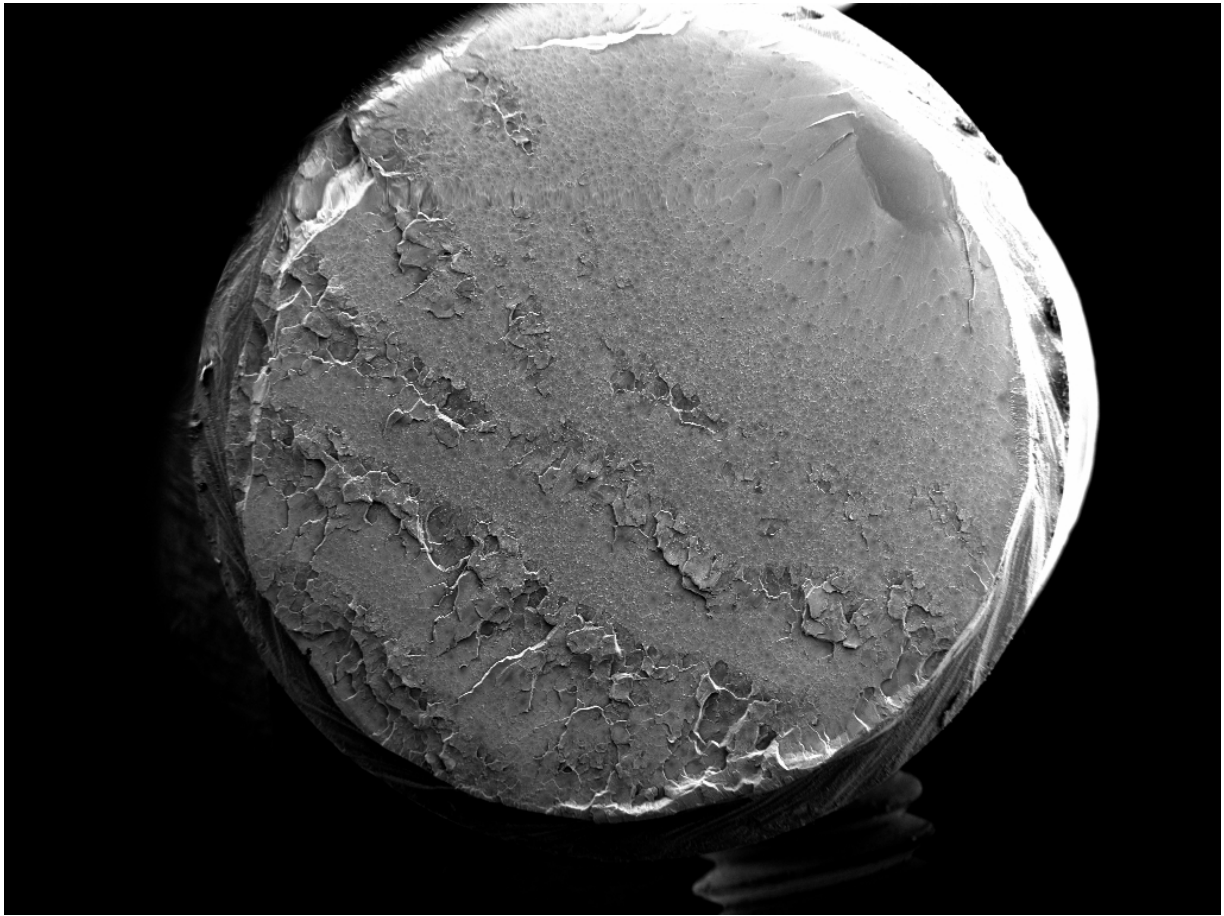
Appendix A1 (Bridgman experiment, fracture surface PMMA):



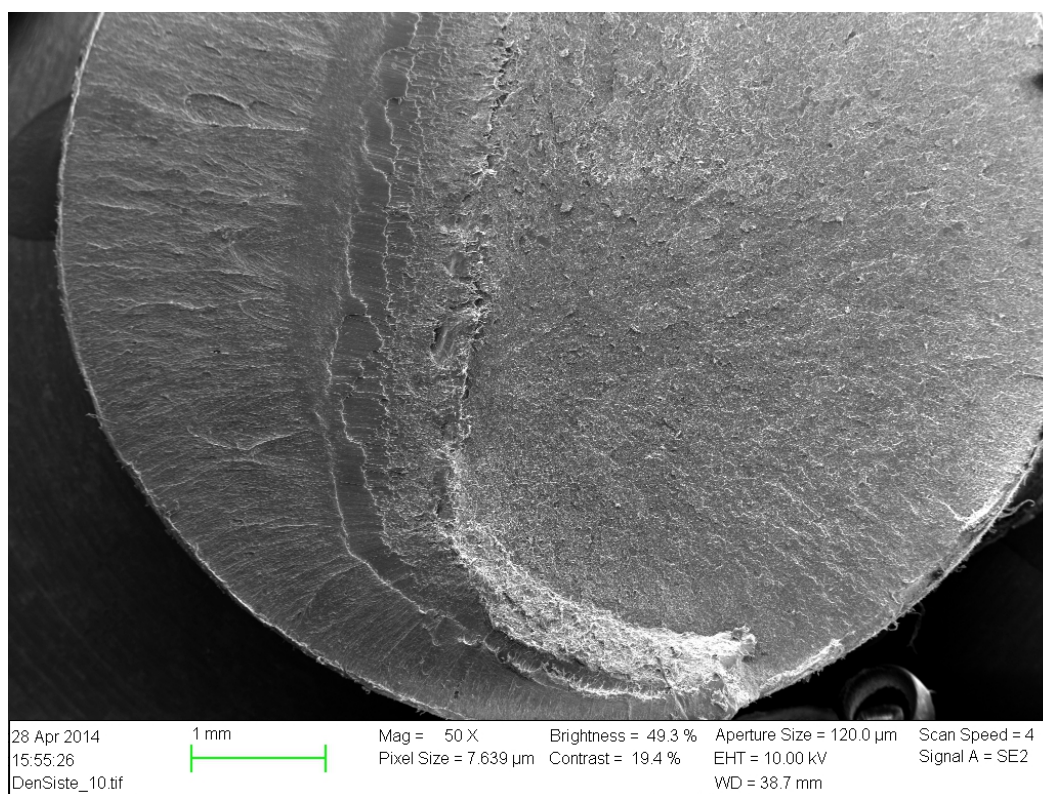
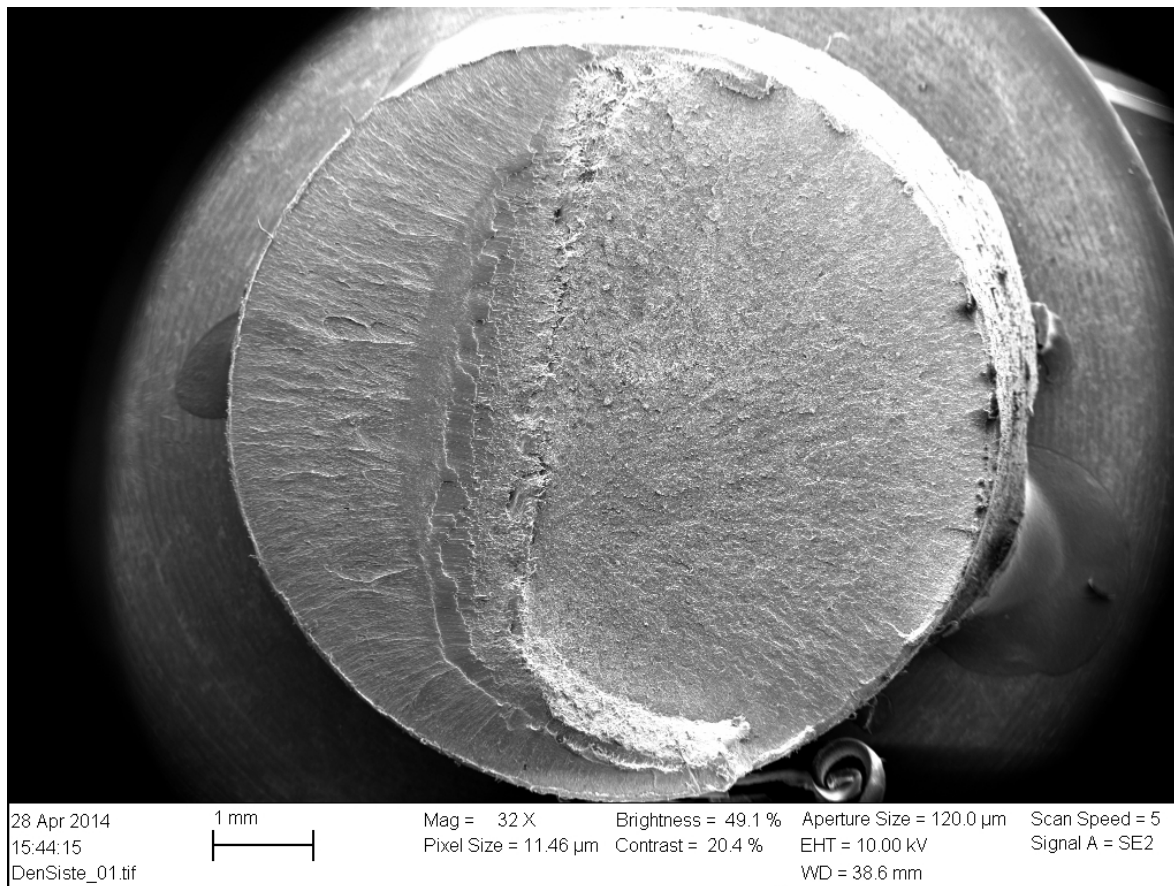
Appendix A2 (Bending experiment, fracture surface PMMA):



Appendix A3 (Tension loading, fracture surface PMMA):



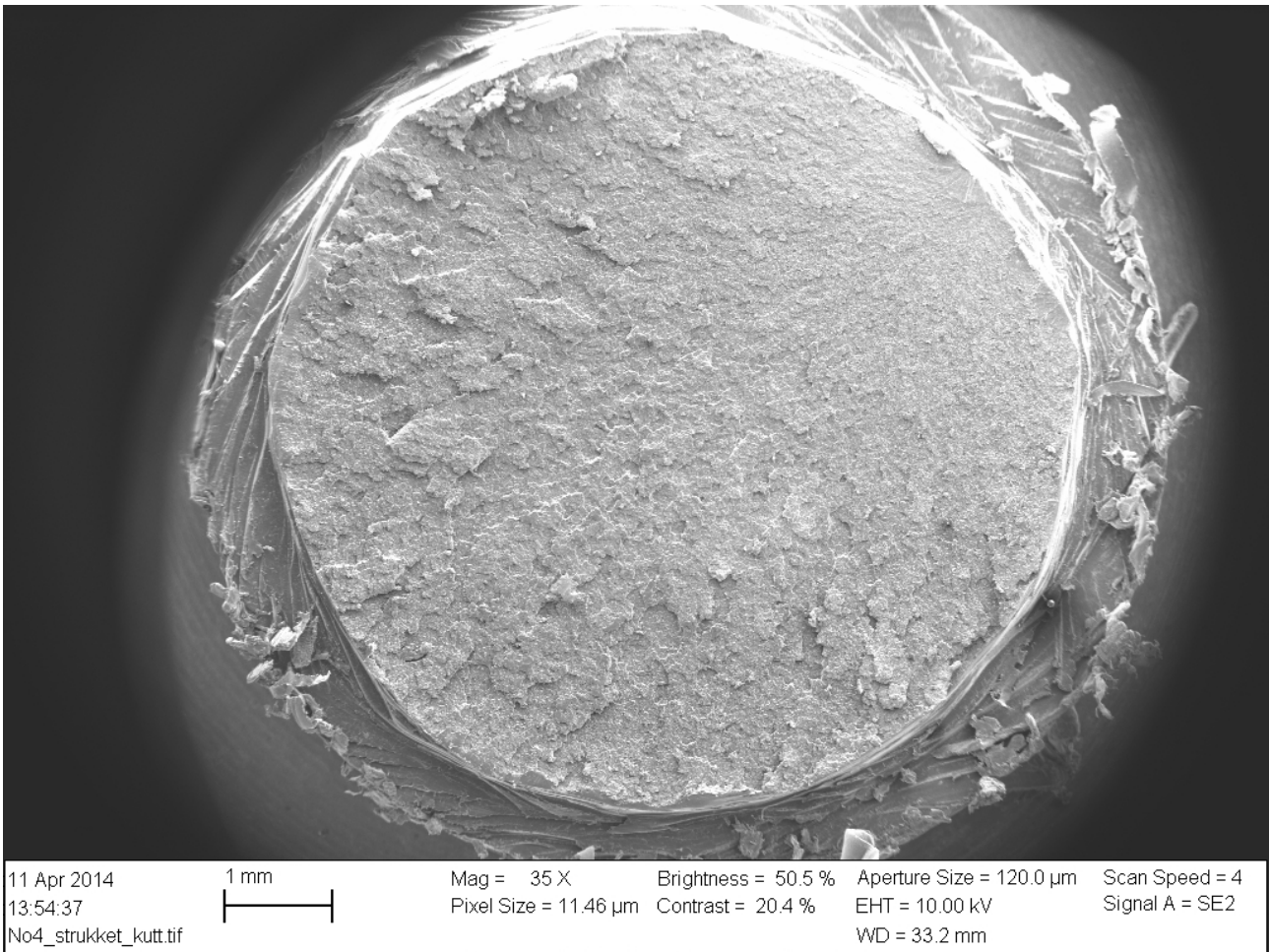
Appendix A4 (Bridgman experiment, fracture surface POM-C):



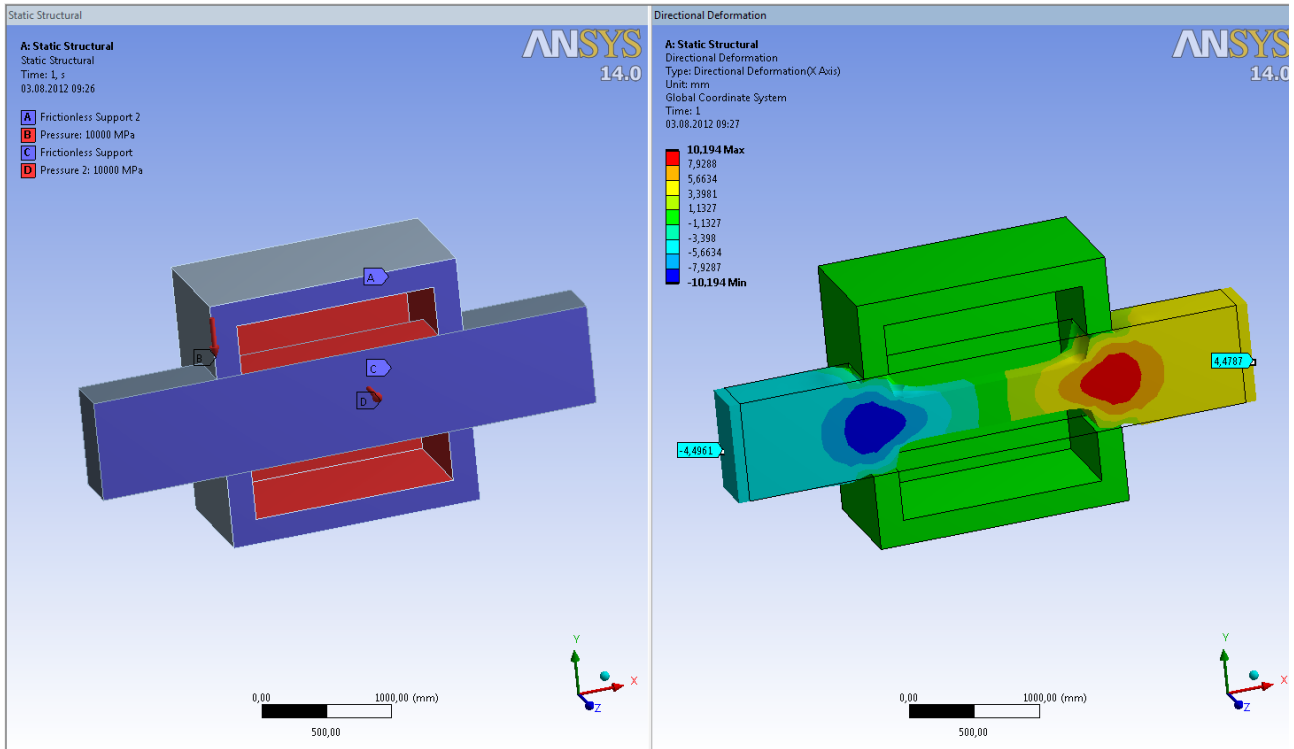
Appendix A5 (Bending experiment, fracture surface POM-C):



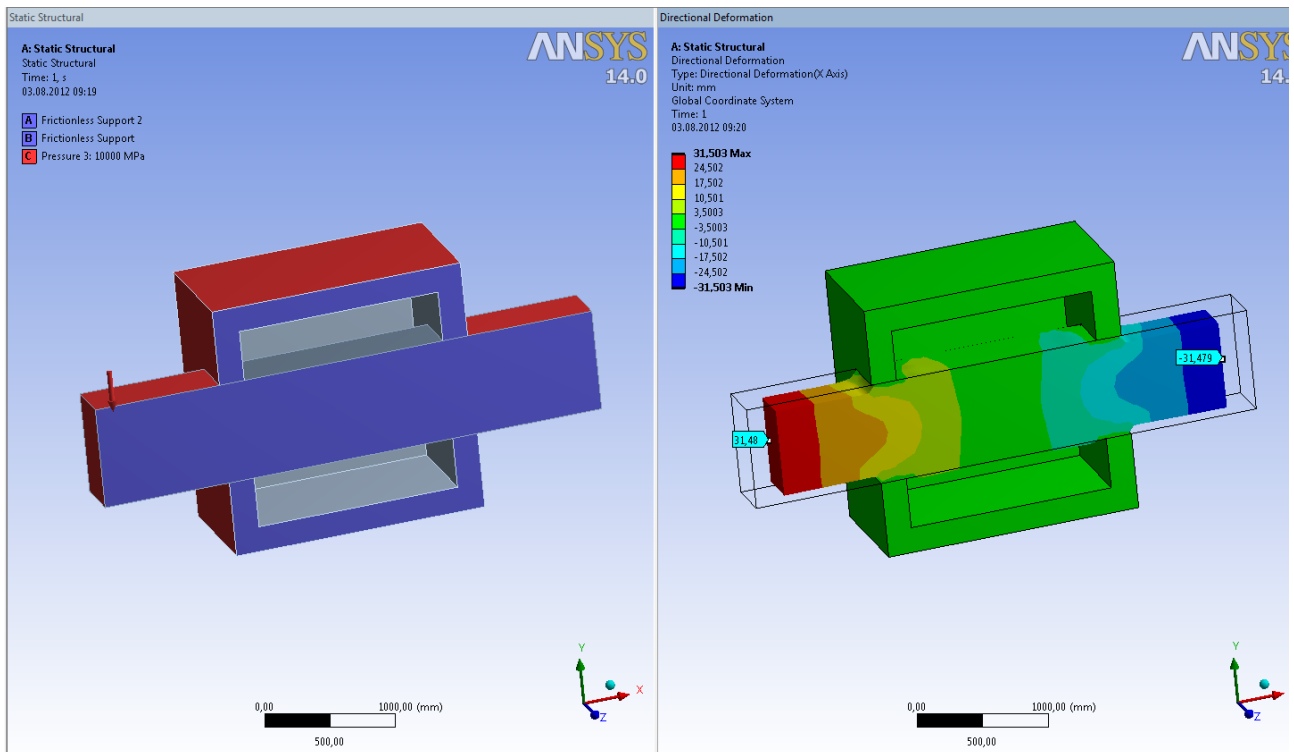
Appendix A6 (Tension loading, fracture surface POM-C):



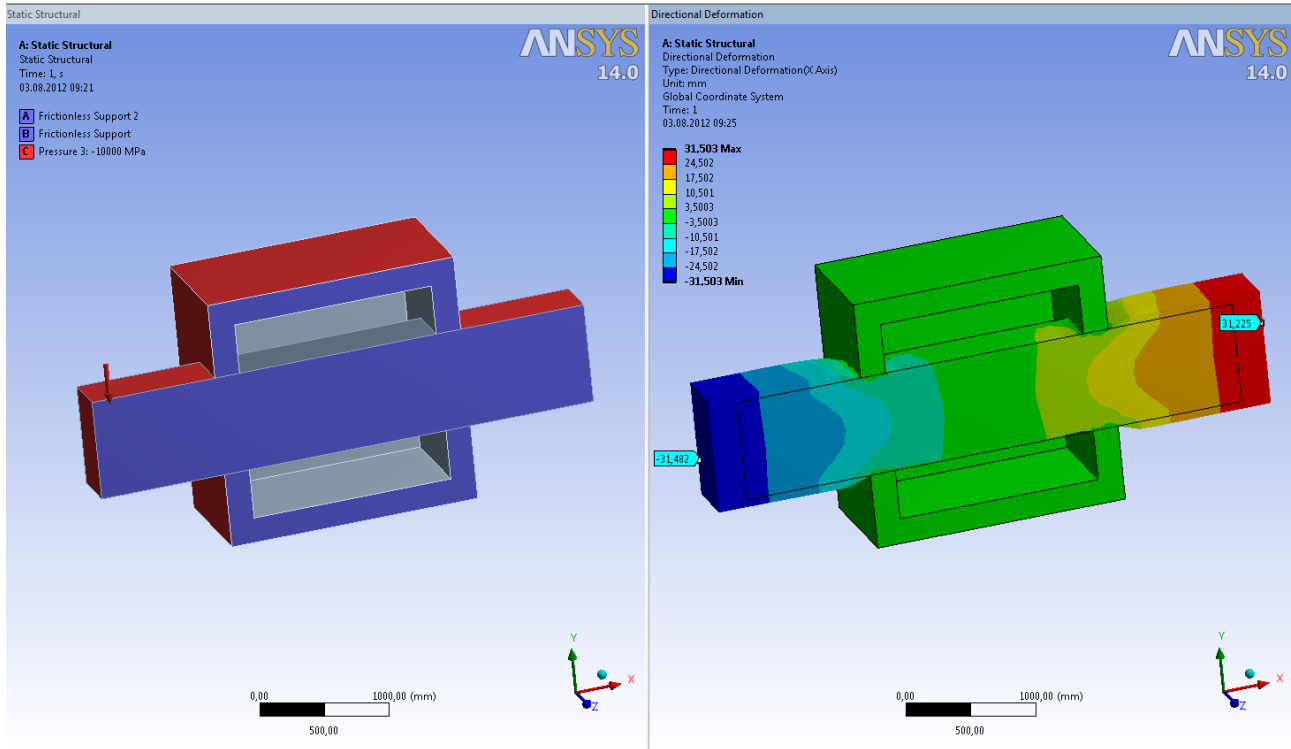
Appendix B1 (Ansys model, inside pressure):



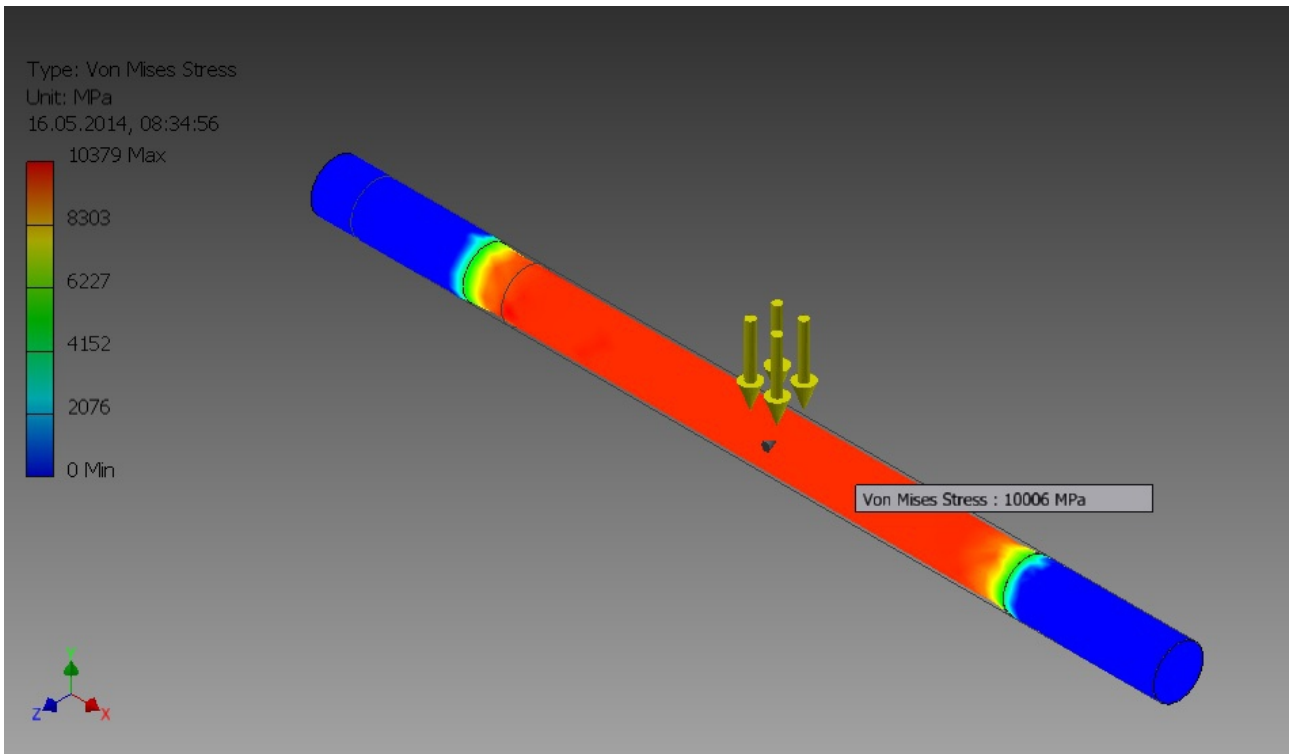
Appendix B2 (Ansys model, outside pressure):



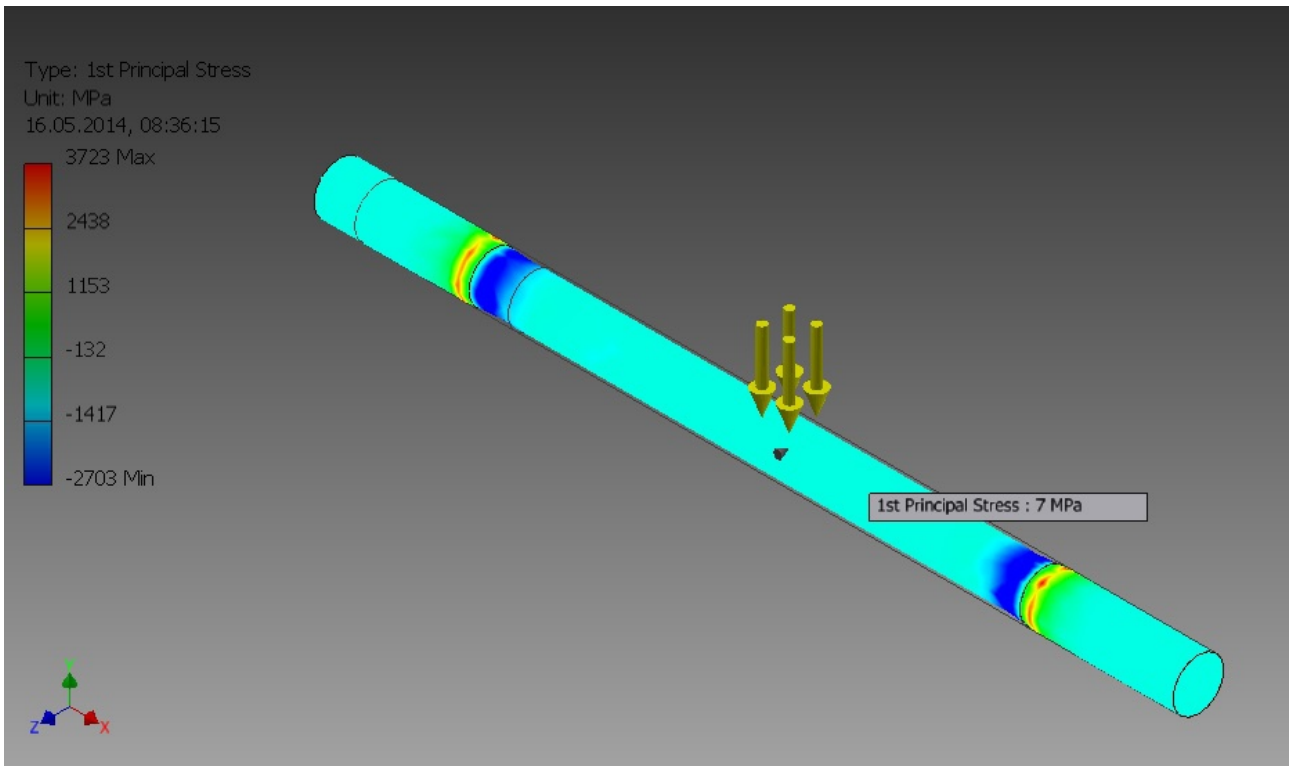
Appendix B3 (Ansys model, outside negative pressure):



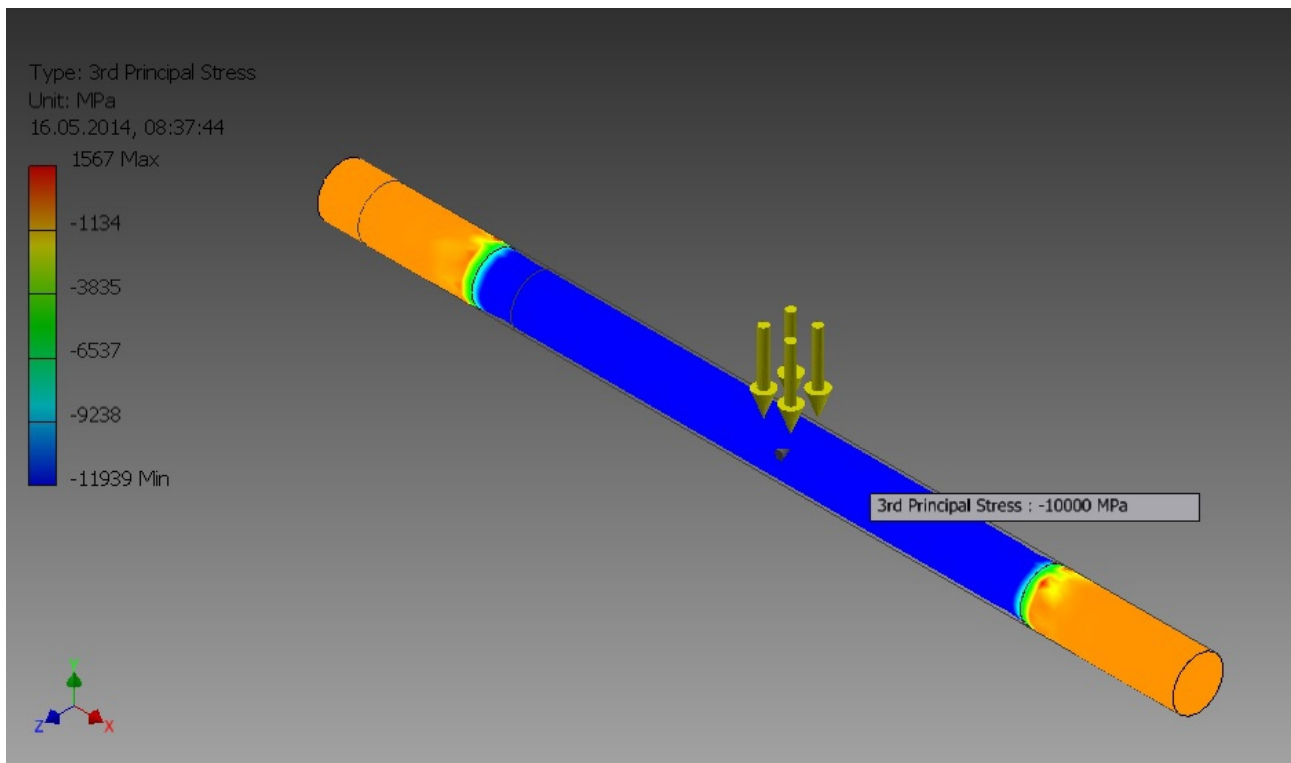
Appendix C1.1 (Inventor model, inside pressure. Von Mises stress):



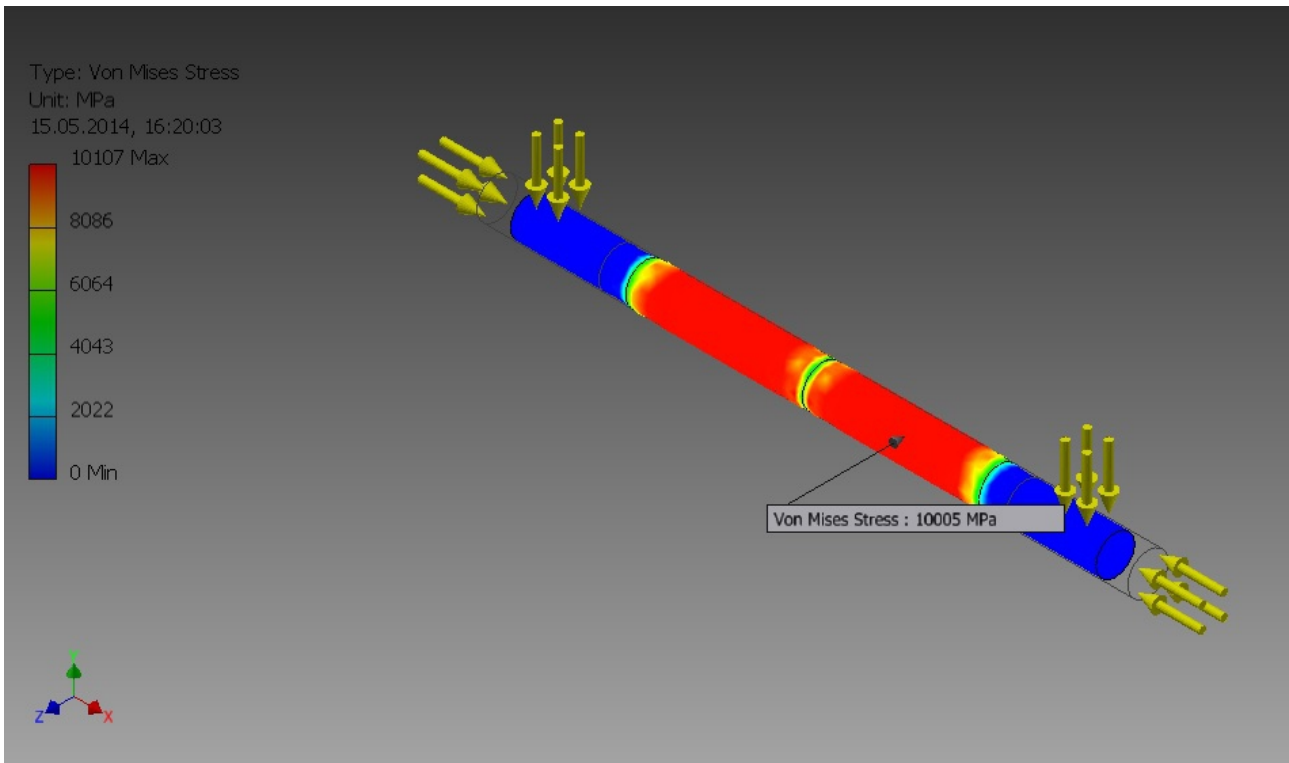
Appendix C1.2 (Inventor model, inside pressure. 1st principal stress):



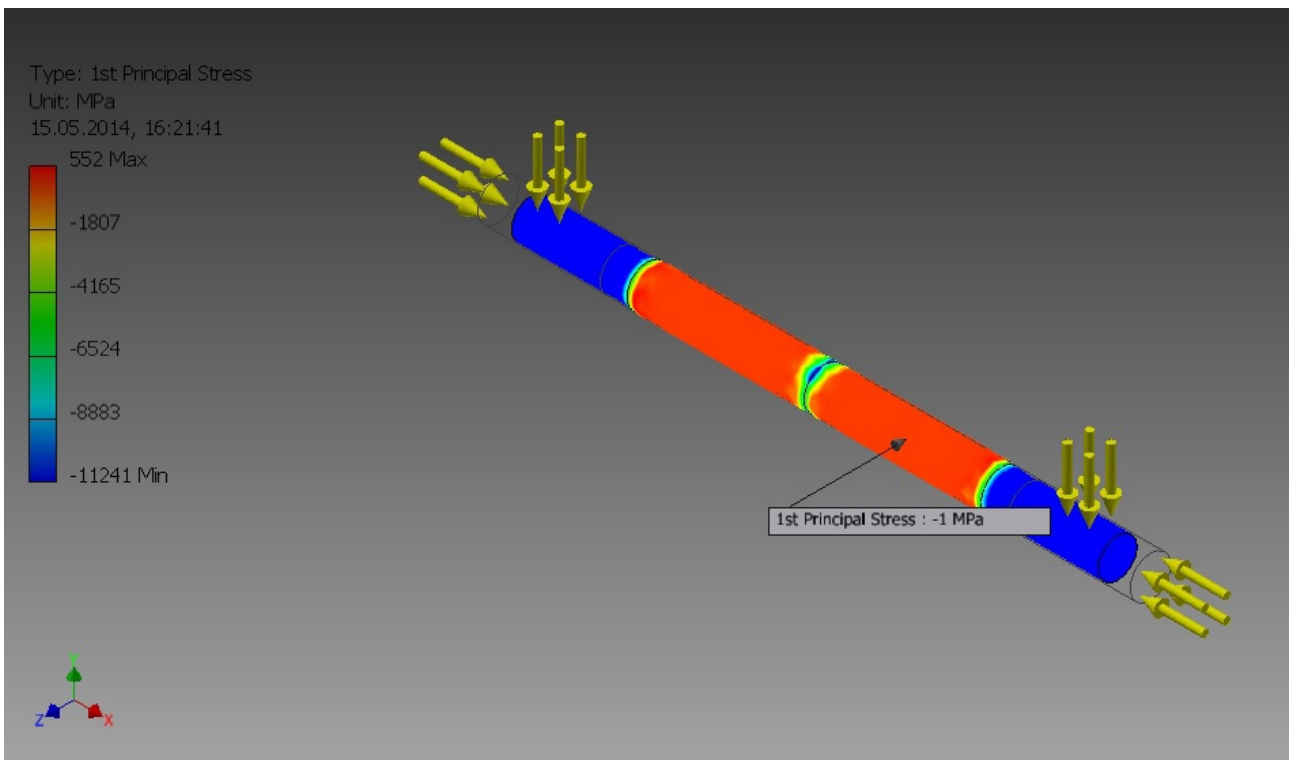
Appendix C1.3 (Inventor model, inside pressure. 3rd principal stress):



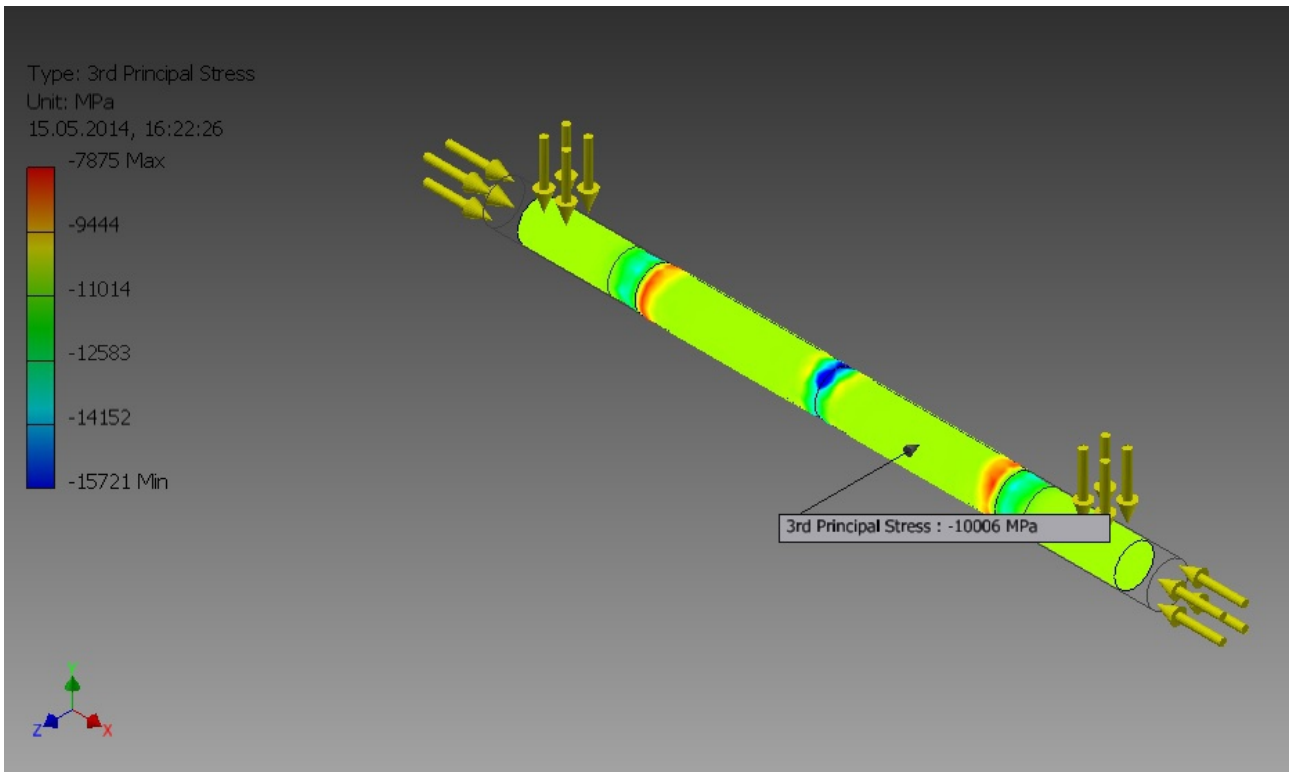
Appendix C2.1 (Inventor model, outside pressure. Von Mises stress):



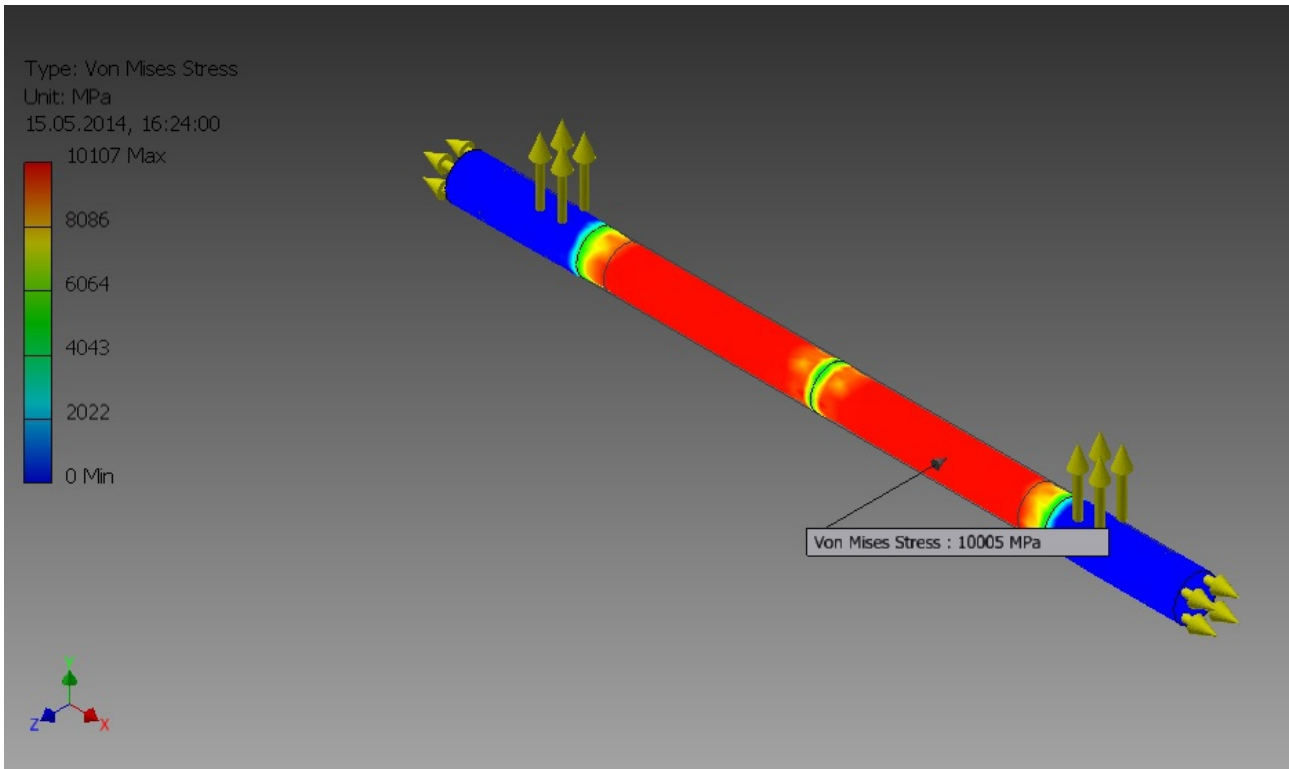
Appendix C2.2 (Inventor model, outside pressure. 1st principal stress):



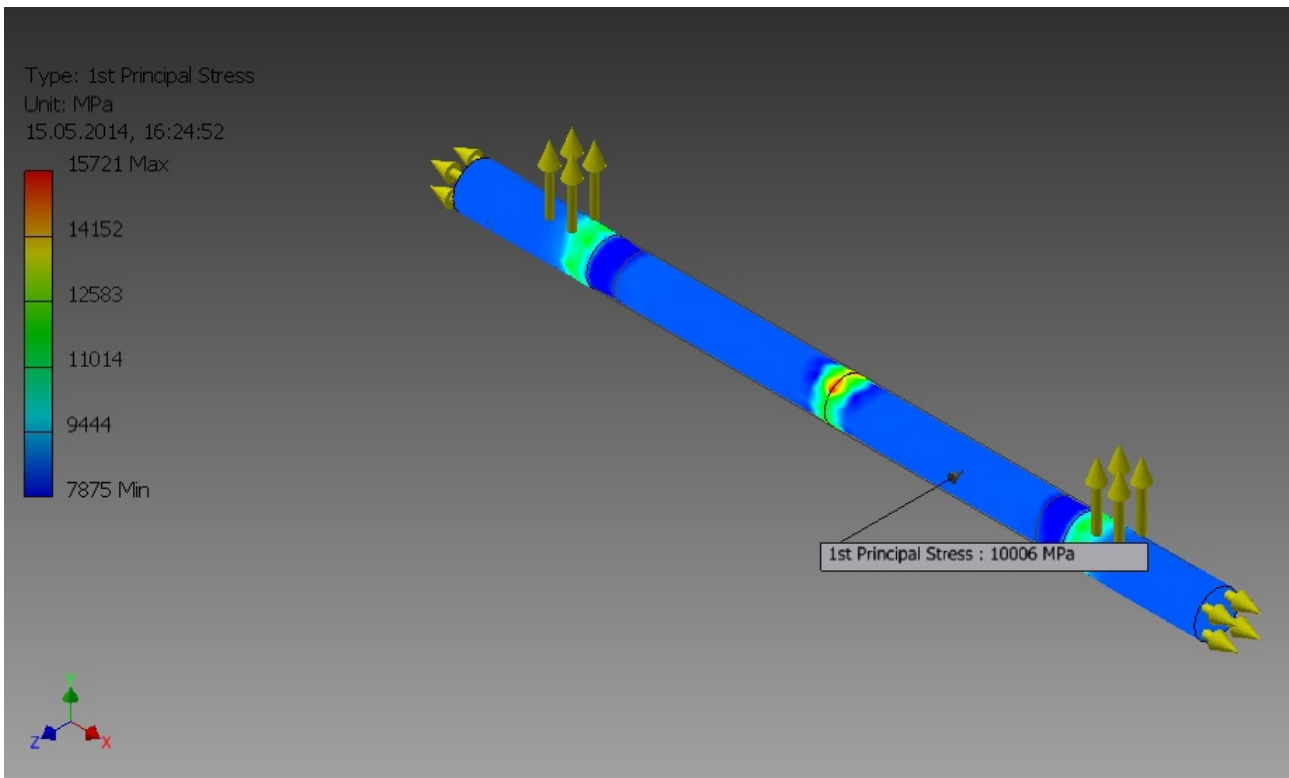
Appendix C2.3 (Inventor model, outside pressure. 3rd principal stress):



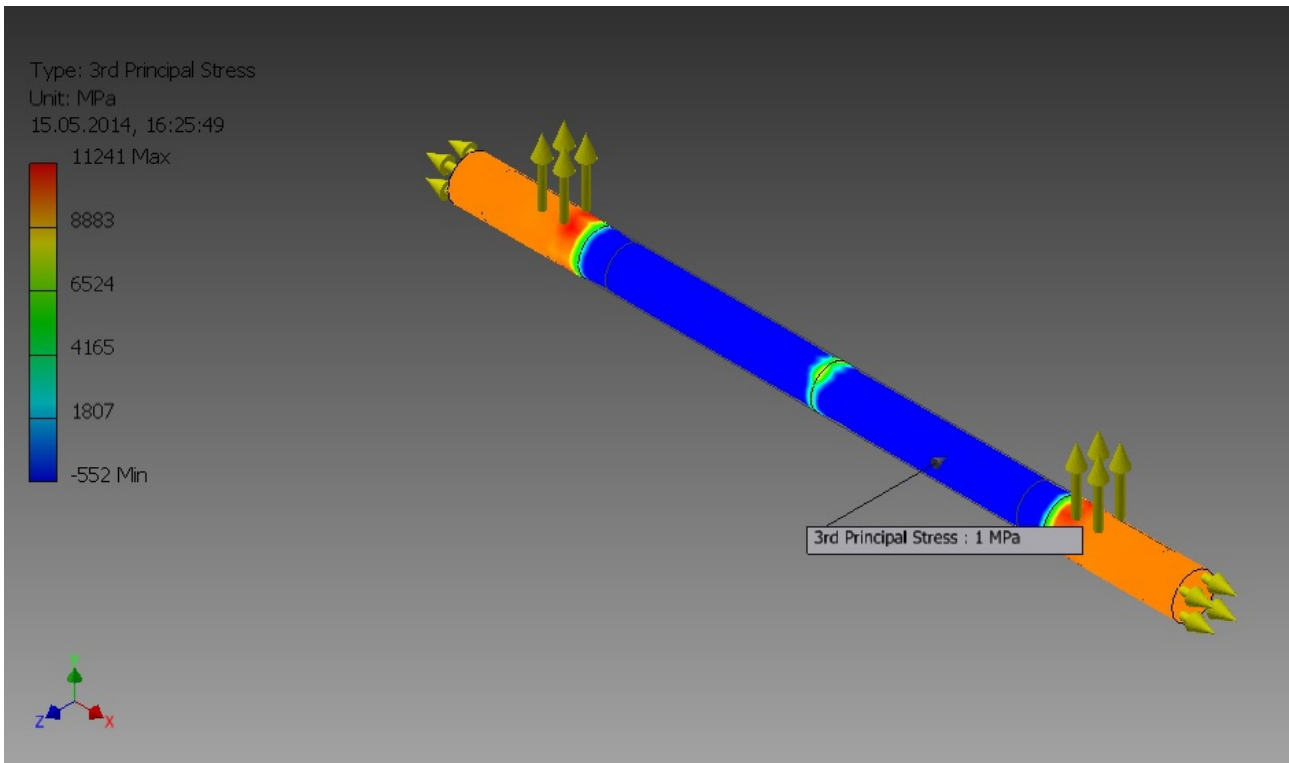
Appendix C3.1 (Inventor model, outside negative pressure. Von Mises stress):



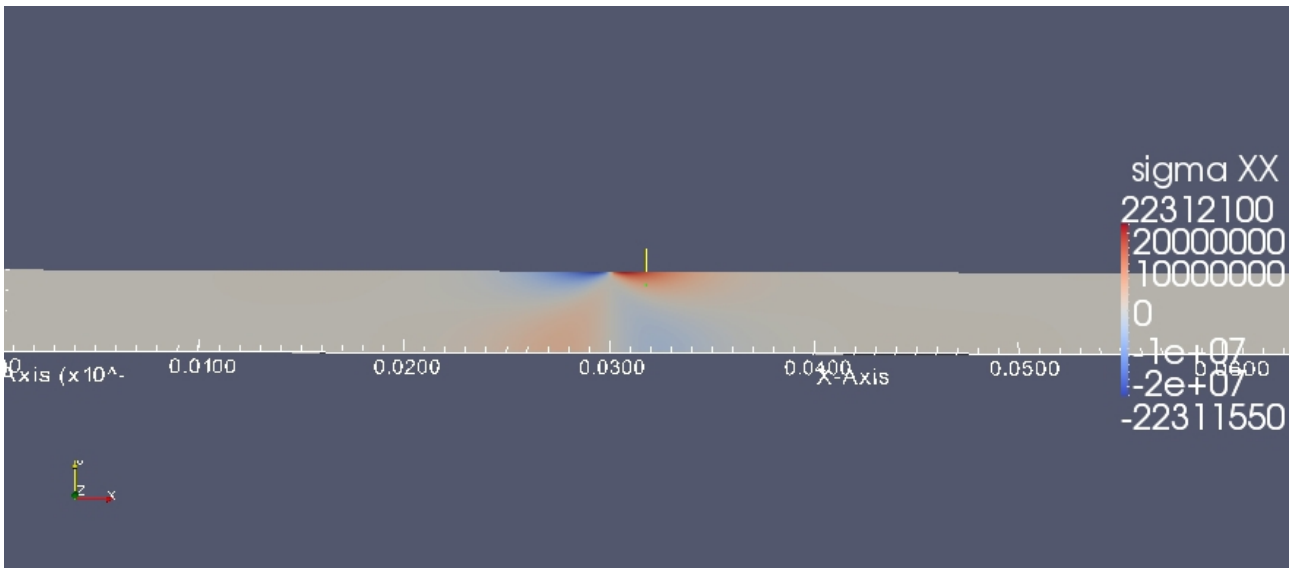
Appendix C3.2 (Inventor model, outside negative pressure. 1st principal stress):



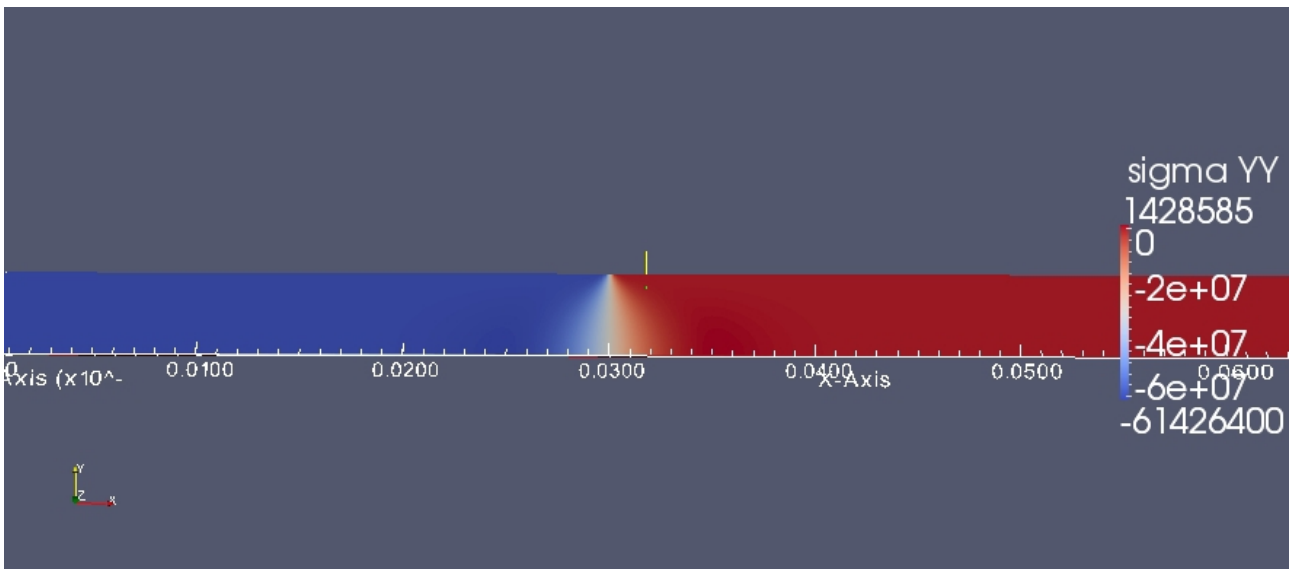
Appendix C3.3 (Inventor model, outside negative pressure. 3rd principal stress):



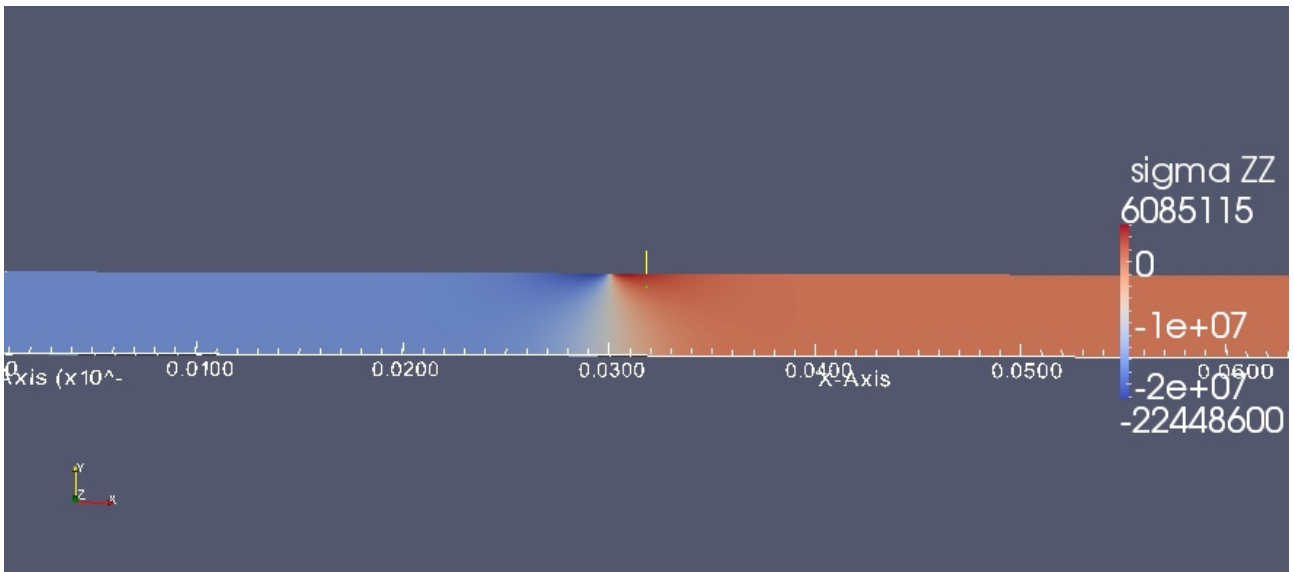
Appendix D1 (OpenFOAM model, inside pressure. Stress in X-direction):



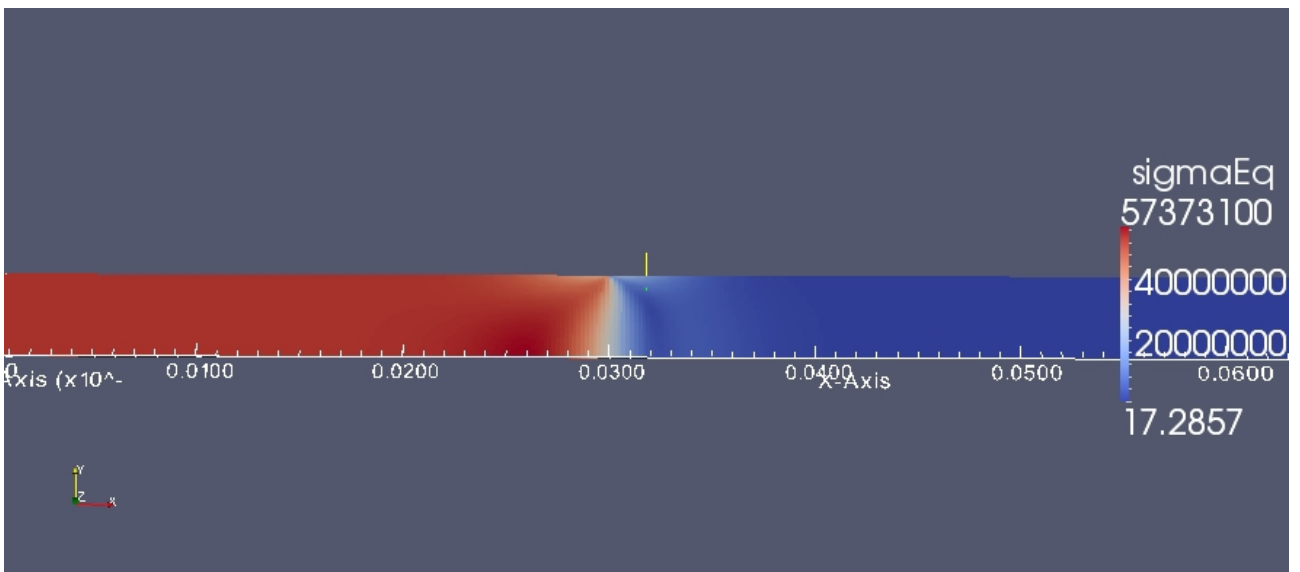
Appendix D2 (OpenFOAM model, inside pressure. Stress in Y-direction):



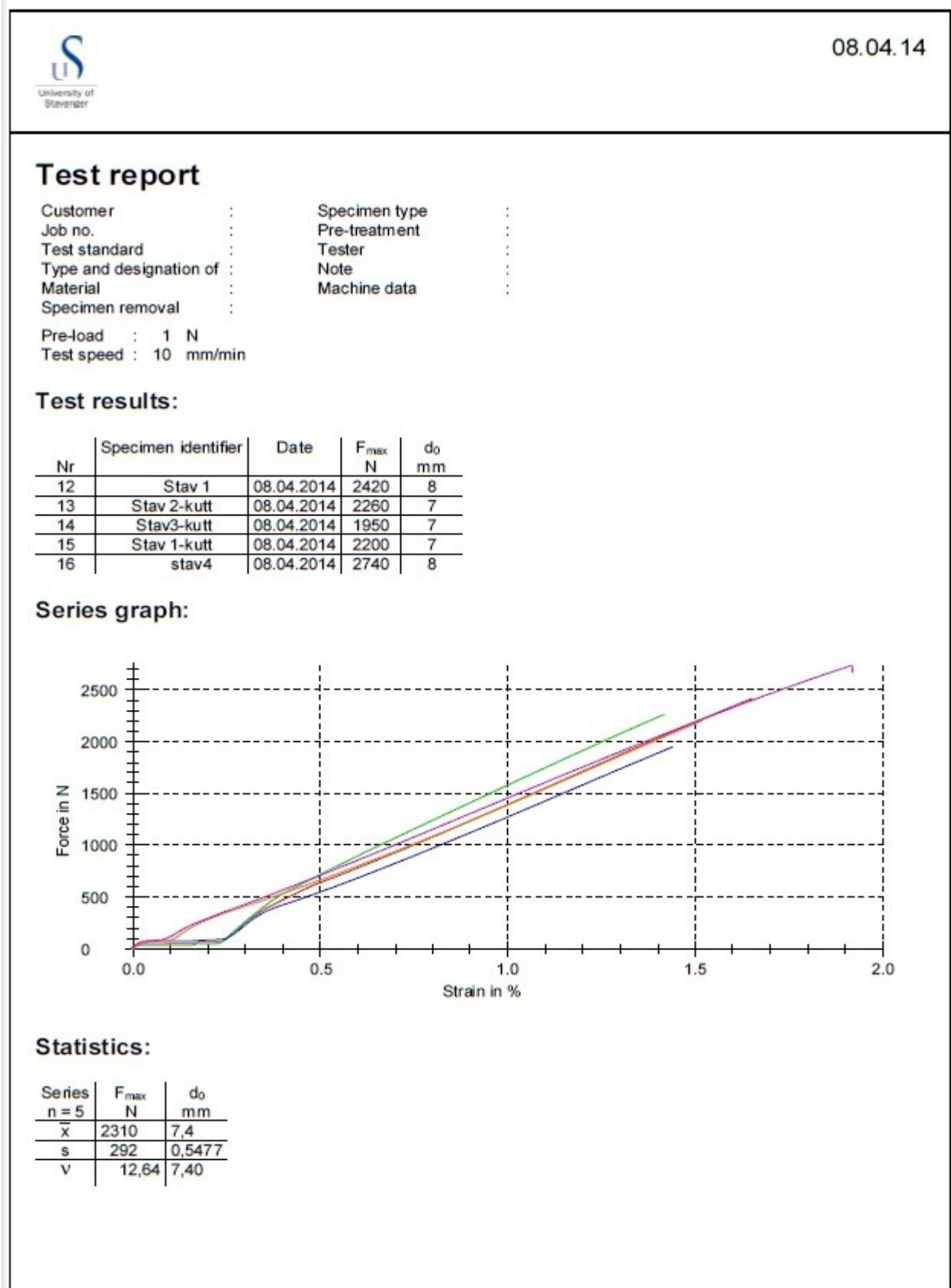
Appendix D3 (OpenFOAM model, inside pressure. Stress in Z-direction):



Appendix D4 (OpenFOAM model, inside pressure. Von Mises stress):



Appendix E (Tension experiment. Stress and strain plotting):



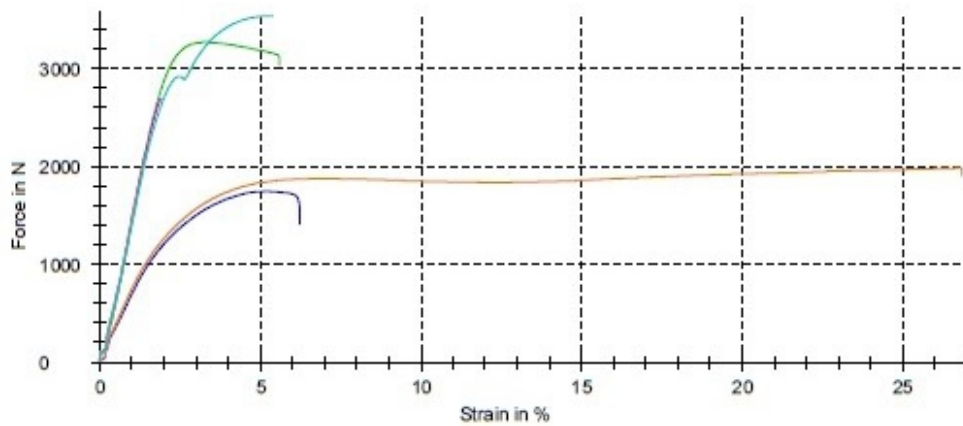
Test report

Customer : Specimen type :
 Job no. : Pre-treatment :
 Test standard : Tester :
 Type and designation of : Note :
 Material : Machine data :
 Specimen removal :
 Pre-load : 5 N
 Test speed : 20 mm/min

Test results:

Nr	Specimen identifier	Date	F _{max} N	d ₀ mm
17	Stav-svart hakk	10.04.2014	2210	6,5
18	Stav-svart	10.04.2014	3270	8,4
19	Stav-grå hakk	10.04.2014	1740	7,2
20	Stav-grå	10.04.2014	1980	8,4
21	Stav-hvit hakk	10.04.2014	2690	6,9
22	Stav-hvit	10.04.2014	3540	8,4

Series graph:



Statistics:

Series	F _{max} N	d ₀ mm
n = 6		
x	2570	7,633
s	721	0,8687
v	28,02	11,38

Appendix F (200x, 2000x and 5000x surface of PMMA rod):

